New Jersey Geological Survey
Geological Survey Report GSR 37

GEOPHYSICAL INVESTIGATION OF THE POTOMAC-RARITAN-MAGOTHY AQUIFER SYSTEM AND UNDERLYING BEDROCK IN PARTS OF MIDDLESEX AND MERCER COUNTIES, NEW JERSEY

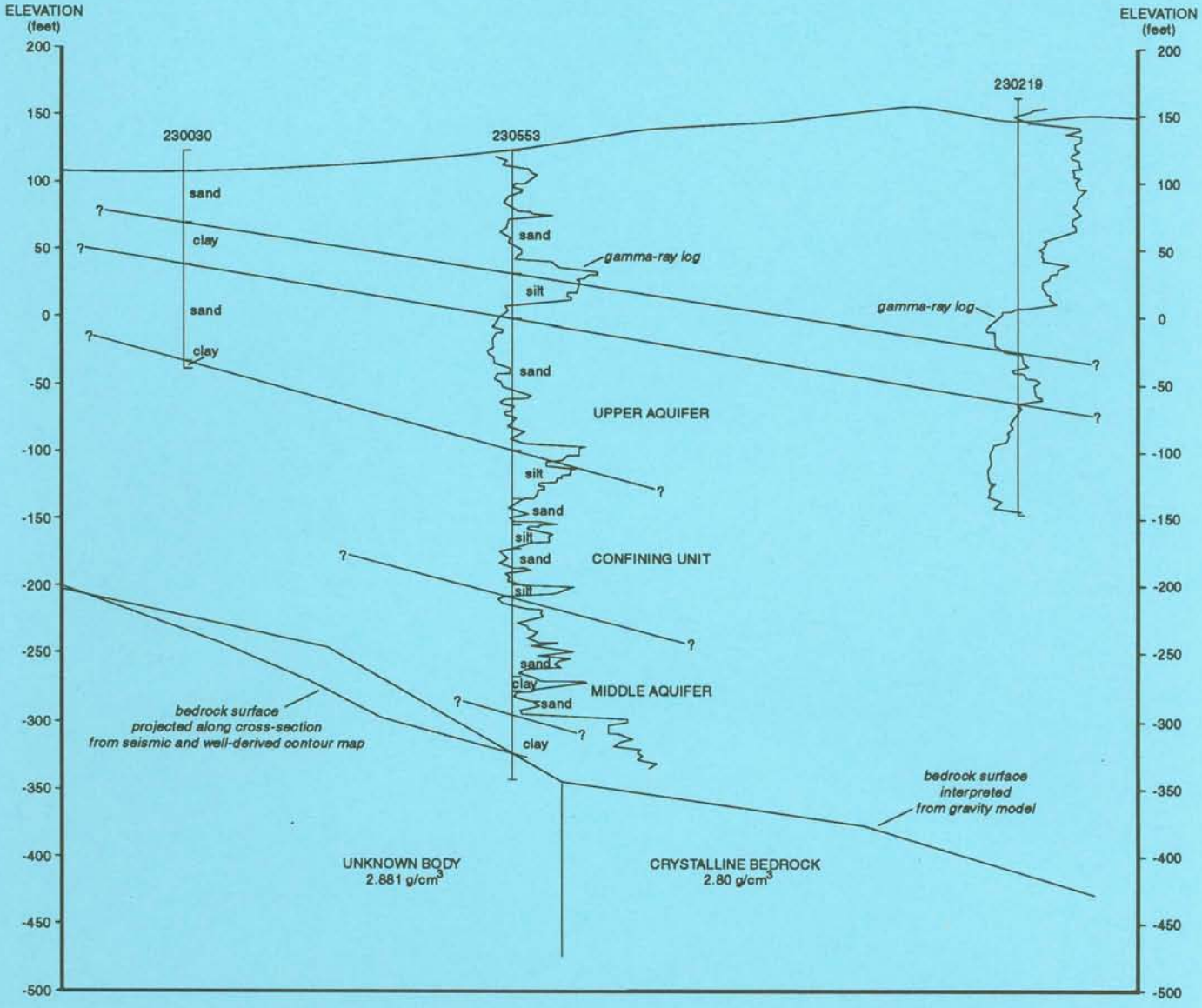

N.J. Department of Environmental Protection - Division of Science and Research

New Jersey Geological Survey
Geological Survey Report GSR 37

Geophysical Investigation of the Potomac-Raritan-Magothy Aquifer System and Underlying Bedrock in Parts of Middlesex and Mercer Counties, New Jersey

by
Stewart K. Sandberg[1, 2]
David W. Hall[1]
Jo Ann M. Gronberg[3]
David L. Pasicznyk[1]

[1] New Jersey Geological Survey
Trenton, NJ

[2]Current address:
University of Southern Maine
Geoscience Department
37 College Avenue
Gorham, ME, 04038

[3] U.S. Geological Survey
Water-Resources Division
Mountain View Office Park
810 Bear Tavern Road
West Trenton, NJ 08628

New Jersey Department of Environmental Protection
Division of Science and Research
Geological Survey
CN 427
Trenton, NJ 08625
1996

Printed on recycled paper

New Jersey Geological Survey Reports (ISSN 0741-7357) are published by the New Jersey Geological Survey, CN 427, Trenton, NJ 08625.

Additional copies of this and other reports may be obtained from:

Maps and Publications Sales Office
Bureau of Revenue
CN 417
Trenton, NJ 08625

A price list is available on request.

Use of brand, commercial, or trade names is for identification purposes only and does not constitute endorsement by the New Jersey Geological Survey.

CONTENTS

ILLUSTRATIONS

PLATES

TABLES

Geophysical Investigation of the Potomac-Raritan-Magothy Aquifer System and Underlying Bedrock in Parts of Middlesex and Mercer Counties, New Jersey

ABSTRACT

Surface geophysical techniques were used in conjunction with geophysical and lithologic well logs to map the Potomac-Raritan-Magothy aquifer system and bedrock lithology in an area extending from Plainsboro to Perth Amboy in central New Jersey. The surface geophysical techniques included seismic reflection and refraction, electrical resistivity, induced polarization, gravity, and magnetics.

Geophysical data allowed the delineation of (1) an aquifer pinch-out coincident with a bedrock high due east of Sayreville, (2) termination of the Woodbridge clay confining unit within the Hightstown quadrangle, probably due to a facies change from clayey silt to sand, (3) the boundary between crystalline basement and Newark Supergroup sedimentary bedrock, (4) the subsurface extension of the Palisades diabase sill, and (5) a previously unknown dense rock body with high magnetic susceptibility within the crystalline bedrock.

INTRODUCTION

In the Atlantic Coastal Plain of New Jersey, ground water is the major source of water supply. Due to increased withdrawals of ground water in recent years, significant regional cones of depression have developed. Declining water levels have caused saltwater intrusion in the middle aquifer of the Potomac-Raritan-Magothy aquifer system in Sayreville Borough and South Amboy City (Schaefer, 1983, p. 11) and in other aquifers elsewhere along the New Jersey coast.

To evaluate the potential for serious damage to Coastal Plain water resources, regional investigations have been undertaken in the Atlantic City, Camden, and South River areas (Leahy and others, 1987). This report is one of a series of products originating from the South River regional ground-water investigation, a cooperative effort between the New Jersey Geological Survey (NJGS) and the U.S. Geological Survey - Water Resources Division. It was funded by the New Jersey Water Bond Issue of 1981. The Potomac-Raritan-Magothy aquifer system is the most productive source of potable water in the area and is, therefore, the main focus of the South River regional study.

This portion of the study provides results of a surface geophysical investigation designed to improve understanding of the hydrogeologic framework in the South River area. Specific contributions were (1) evaluation of the continuity of the confining unit separating the upper and middle aquifers of the Potomac-Raritan-Magothy aquifer system, (2) discovery of the effect of bedrock topography on the thickness of the middle aquifer, (3) refinement of the delineation of the boundaries of the Palisades sill subcrop beneath the Coastal Plain sediments, and (4) an improved knowledge of bedrock structure.

All data in this study were interpreted by computer modeling methods which simulate geologic relationships so as to be consistent with geophysical measurements. The results are shown in 12 interpretative cross sections and 2 bedrock topography maps (pls. 1-3).

Location and extent of study area

The study area (fig. 1) lies within Mercer and

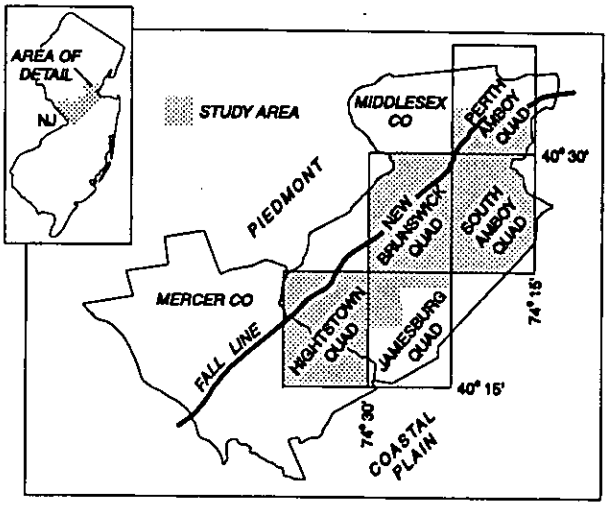

Figure 1. Location of study area and fall line.

Middlesex Counties and consists of the Hightstown, New Brunswick, South Amboy, and parts of the Perth Amboy, and Jamesburg U.S. Geological Survey 7.5-minute quadrangles. The area straddles the Fall Line, which separates bedrock of the Piedmont Physiographic Province from unconsolidated sediments of the Atlantic Coastal Plain.

Well-numbering system

The method used for well-numbering in this report is based on a system used by the U. S. Geological Survey for its Ground-Water Site Inventory (GWSI). The first two digits of the well number are the county code; in this report well numbers for Mercer County begin with 21, those for Middlesex County with 23. The numbers were assigned sequentially as the wells were entered into the GWSI system.

Table 6 cross-references New Jersey Bureau of Water Allocation well permit numbers and GWSI well numbers used in this report. A compilation of borehole geophysical and drillers' logs for wells used in this study can be found in Gronberg and others (1989).

ACKNOWLEDGMENTS

The authors thank Suhas L. Ghatge, Jeffrey S. Waldner, Donald L. Jagel, and Thomas C. Bambrick, all at the time of the study with NJGS, for assistance with field work. In addition, we thank Dr. Robert E. Sheridan of Rutgers University, Amletto A. Pucci, formerly of the U.S. Geological Survey - Water Resources Division, and Richard Dalton of NJGS, for reviewing the manuscript and suggesting improvements. We also thank David Harper and Thomas Seckler for their careful editing, and Zehdreh Allen-Lafayette, Maryann Scott and Bill Graff for their work on the plates and figures. At the time of their participation, all were with NJGS.

GEOLOGIC SETTING

Crystalline bedrock, the oldest rock in the study area, includes Proterozoic gneiss, Wissahickon schist (of controversial, but probably late Proterozoic to Early Paleozoic age), granitic and gabbroic intrusives, and possibly, altered diabase (Ghatge and others, 1989).

Unconformably overlying the crystalline bedrock are sedimentary and igneous rocks of the Newark Supergroup. The sedimentary rock consists of sandstone of the Stockton Formation, argillite of the Lockatong Formation, and shale of the Passaic Formation, all of Triassic age. The igneous bedrock consists of the subcrop extension of the Palisades diabase sill of Jurassic age.

Unconformably overlying the Newark Supergroup are unconsolidated Cretaceous, Paleocene, Eocene, Miocene, and Pleistocene sediments (tables 1 and 2). Within the Coastal Plain sediments, the Potomac Group and the Raritan and Magothy Formations compose the Potomac-Raritan-Magothy aquifer system. The Potomac Group consists of alternating clay, silt, sand, and gravel deposited under continental conditions by meandering streams (Owens and Gohn, 1985, p. 41). In this report, individual formations were not traced within the Potomac Group in New Jersey, and the sediments are considered a single unit (Owens and others, 1977). Unconformably overlying the Potomac Group is the Raritan Formation, which consists of clays and sands deposited under a wide variety of conditions in a subaerial deltaic plain (Owens and Sohl, 1969, p. 239). Unconformably overlying the Raritan Formation is the Magothy Formation, which consists largely of coarse beach sand and associated marine and lagoonal sediments (Gronberg and others, 1991).

The Potomac-Raritan-Magothy aquifer system is divided into lower, middle, and upper aquifers. Only the middle and upper aquifers occur within the study area (Gronberg and others, 1991). The middle aquifer is primarily composed of the Farrington Sand of the Raritan Formation. The confining unit between the middle and upper aquifers consists primarily of the Woodbridge Clay Member of the Raritan Formation. The upper aquifer consists primarily of the Old Bridge Sand member of the Magothy Formation (tables 1 and 2).

Unconformably overlying the Magothy is the Merchantville Formation. This marine deposit consists of massive, thick glauconite sands and thin beds of very micaceous, carbonaceous clayey silt. Conformably overlying the Merchantville is the Woodbury Formation, a thick, massive clayey silt deposited in a marine environment. Together they make up the Merchantville-Woodbury confining layer (Owens and Sohl, 1969, p. 242).

Upper Cretaceous, Paleocene, Eocene, and Miocene sediments overlie the Merchantville-Woodbury

Table 1. Geologic and hydrogeologic units in the Coastal Plain of New Jersey (adapted from New Jersey Geological Survey, 1990)

SYSTEM	SERIES	GEOLOGIC UNIT	LITHOLOGY	HYDROGEOLOGIC UNIT		HYDROGEOLOGIC CHARACTERISTICS
Quaternary	Holocene	alluvial deposits	sand, silt, and black mud	undifferentiated		Surficial material, commonly hydraulically connected to underlying aquifers. Locally some units may act as confining units. Thicker sands are capable of yielding large quantities of water
		beach sand and gravel	sand, quartz, light colored, medium to coarse grained, pebbly			
	Pleistocene	Cape May Formation	sand, quartz, light colored, heterogeneous, clayey, pebbly			
Tertiary	Miocene	Pensauken Formation		Kirkwood-Cohansey aquifer system		A major aquifer system. Ground water occurs generally under water-table conditions. In Cape May County, the Cohansey Sand is under artesian conditions
		Bridgeton Formation				
		Beacon Hill Gravel	gravel, quartz, light colored, sandy			
		Cohansey Sand	sand, quartz, light colored, medium to coarse grained, clayey, pebbly, local clay beds			
		Kirkwood Formation	sand, quartz, gray and tan, very fine to medium grained, micaceous, and dark colored diatomaceous clay	confining unit		Thick diatomaceous clay bed occurs along coast and for a short distance inland. A thin water-bearing sand is present in the middle of this unit
				Rio Grande water-bearing zone		
				confining unit		
				Atlantic City 800-foot sand		A major aquifer along the coast
	Oligocene	unnamed formation	sand, quartz and glauconite, fine- to coarse-grained	Composite confining unit		poorly permeable sediments
					Piney Point aquifer	Confined aquifer. Thin with limited overall potential; brackish downdip
	Eocene	Shark River Formation				poorly permeable sediments
		Manasquan Formation	clay, silty and sandy, glauconitic, green, gray, and brown, fine grained quartz sand		Vincentown aquifer	Moderate to small yields in and near outcrop areas
	Paleocene	Vincentown Formation	sand, quartz, gray and green, fine to coarse grained, glauconitic; glauconite, brown, clayey, very fossiliferous; quartz calcarenite			
		Hornerstown Sand	sand, clayey, glauconitic, dark green, fine to coarse grained			poorly permeable sediments
Cretaceous	Upper Cretaceous	Tinton Sand	sand, quartz and glauconite, brown and gray, fine to coarse grained, clayey, micaceous			
		Red Bank Sand			Red Bank Sand	Moderate to small yields in and near outcrop areas
		Navesink Formation	sand , clayey, silty, glauconitic, green and black, medium to coarse grained			poorly permeable sediments
		Mount Laurel Sand	sand, quartz, brown and gray, fine to coarse grained, slightly glauconitic	Wenonah - Mount Laurel aquifer		A major aquifer
		Wenonah Formation	sand, very fine to fine grained, gray and brown, silty, slightly glauconitic	Marshalltown - Wenonah confining unit		A leaky confining unit
		Marshalltown Formation	clay, silty, dark greenish gray; sand, quartz, glauconitic			
		Englishtown Formation	sand, quartz, tan and gray, fine to medium grained; local clay beds	Englishtown aquifer system		A major aquifer. Two sand units in Monmouth and Ocean Counties
		Woodbury Clay	clay, gray and black, micaceous silt	Merchantville-Woodbury confining unit		A major confining unit. Locally, the Merchantville Formation may contain a thin water-bearing sand.
		Merchantville Formation	clay, glauconitic, gray and black; locally sand, quartz and glauconite, very fine grained			
		Magothy Formation	sand, quartz, light gray, fine to coarse grained; local clay beds, dark gray, lignitic	Potomac-Raritan-Magothy aquifer system	upper aquifer	A major aquifer system. In the northern Coastal Plain, the upper aquifer is equivalent to the Old Bridge aquifer and the middle aquifer is equivalent to the Farrington aquifer. In the Delaware River valley, three aquifers are recognized. In the deeper subsurface, units below the upper aquifer are undifferentiated.
					confining unit	
		Raritan Formation	sand, quartz, light gray, fine to coarse grained, pebbly, arkosic, red, white; clay, variegated		middle aquifer	
					confining unit	
	Lower Cretaceous	Potomac Group	clay, silt, sand, and gravel, alternating		lower aquifer	
Pre-Cretaceous		bedrock	Triassic sandstone, shale, and Jurassic basalt; Lower Paleozoic and Precambrian crystalline rocks (schist and gneiss)	bedrock confining unit		No wells obtain water from these consolidated rocks except along the Fall Line.

confining layer along the southeastern margin of the study area. Quaternary sediments are distributed discontinuously at the land surface throughout the study area. These sediments were not investigated in this study.

Previous Hydrogeologic Studies

The hydrogeology of the South River area has probably been studied more thoroughly than anywhere else in the state. For this reason, only a partial tabulation of hydrogeologic studies is given here. A more detailed compilation is in Gronberg and others (1991).

The earliest hydrogeologic work on the northern Coastal Plain was done by the New Jersey Geological Survey and published in annual reports of the State Geologist (Woolman, 1889-1902; Knapp, 1904; Kummel and Poland, 1910). Epstein (1986) has outlined this early work chronologically.

Subsequent ground-water studies of the Coastal Plain in the vicinity of the South River area include framework studies by Barksdale (1937), and Barksdale and others (1943). Appel (1962) investigated saltwater intrusion into the middle and upper aquifers of the Potomac-Raritan-Magothy aquifer system (the Farrington and Old Bridge Sands). Ground-water flow and the regional hydrogeologic framework were investigated by Farlekas (1979) and Zapecza (1989). Water quality studies include Barton and others (1987), and Harriman and others (1989). An analysis of hydraulic properties of the upper, middle and lower aquifers was done by Pucci and others (1989).

Table 2. Lithologic subdivisions of the Raritan and Magothy Formations and hydrogeologic units in and near the outcrop (adapted from Gronberg and others, 1991, table 2)

SYSTEM	GEOLOGIC UNIT		LITHOLOGY	HYDROGEOLOGIC UNIT	
Cretaceous	Magothy Formation	Cliffwood beds	sand, quartz, light-gray, fine to coarse grained, local beds of dark gray lignitic clay	Potomac-Raritan-Magothy aquifer system	confining unit
		Morgan beds			
		Amboy Stoneware Clay Member			
		Old Bridge Sand Member			upper aquifer[1]
	Raritan Formation	South Amboy Fire Clay Member	sand, quartz, light gray, fine to coarse grained, pebbly, arkosic; clay, red, white, variegated; saprolitic clay on bedrock		confining unit
		Sayreville Sand Member			
		Woodbridge Clay Member			
		Farrington Sand Member			middle aquifer
		Raritan Fire Clay			confining unit
Pre-Cretaceous	bedrock	bedrock	Triassic sandstone, shale, and Jurassic basalt; Lower Paleozoic and Precambrian crystalline rocks (schist and gneiss)	bedrock confining unit	

[1] Locally, the upper aquifer can include the Sayreville Sand Member where the South Amboy Fire Clay Member is thin or absent.

PREVIOUS GEOPHYSICAL INVESTIGATIONS

Many geophysical investigations have been conducted within the study area. Ewing and others (1939) discussed the "Plainsboro fault block," based on seismic refraction and supported by borehole information and magnetic field intensity measurements.

Woollard (1941), using magnetic vertical-field-intensity contours and seismic refraction, traced the Palisades diabase subcrop beneath Coastal Plain sediments. He also showed the correlation between magnetic anomalies and differential cooling units within the diabase.

Meier (1949) built upon Woollard's network, establishing more than 200 new gravity and magnetic stations in the area. He noticed that the pattern of gravity values parallels the strike of regional tectonic structures. An offset in gravity values was interpreted as a displacement in the basement rocks caused by unequal thrusting and development of a tear fault.

Hickok (1954) interpreted seismic refraction results to produce a bedrock contour map of the pre-Cretaceous rock surface in an area near Lake Carnegie. Varrin (1957) and Carruthers (1959) examined pre-Cretaceous drainage patterns using seismic data to supplement well information from the area.

Fiske (1955) collected data from 93 gravity stations, 179 magnetic stations, and 15 seismic refraction locations. Using this new information, he refuted the Plainsboro fault block interpretation of Ewing and others (1939). Fiske interpreted an erosional feather edge of the Newark Supergroup sediments to explain the offset in Ewing's seismic refraction time-distance curve. He also dismissed the tear fault postulated by Meier (1949).

Dudley (1960) did the first significant electrical geophysical work in the area, collecting 21 Wenner array resistivity soundings. He built upon Fiske's (1955) work and attempted to locate the Newark Supergroup feather edge using the resistivity method.

Runyan (1961) also built upon Fiske's 1955 work, collecting another 16 seismic refraction profiles. Runyan reinterpreted and incorporated data from the previous Princeton University seismic investigations (Carruthers, 1959; Dudley, 1960; Varrin, 1957; Fiske, 1955; and Hickok, 1954) and generated a bedrock contour map of the Kingston-Plainsboro-Monmouth Junction area.

Methodology, preliminary findings, and selected data from the present study were published by Sandberg and Hall (1990).

GEOPHYSICAL METHODS

Seismic Refraction and Reflection

Seismic data were collected to delineate the bedrock surface and lithologic units within the Coastal Plain sediments. Data were collected at 40 locations (pls. 1, 3; tables 3, 4). Seismic refraction was used at most locations; however, seismic reflection was substituted where cultural development precluded adequate line length for the refraction method (fig. 2).

Geologic conditions in the study area were favorable for use of seismic methods. The Coastal Plain sediments are essentially flat-lying, dipping very gently to the southeast at 10 to 60 ft/mi (Zapecza, 1989, p. B5). Consequently, errors related to regional dip are small or negligible for the 220- to 550-foot geophone spread lengths used. Seismic velocities were always much higher in bedrock than in overlying unconsolidated sediments.

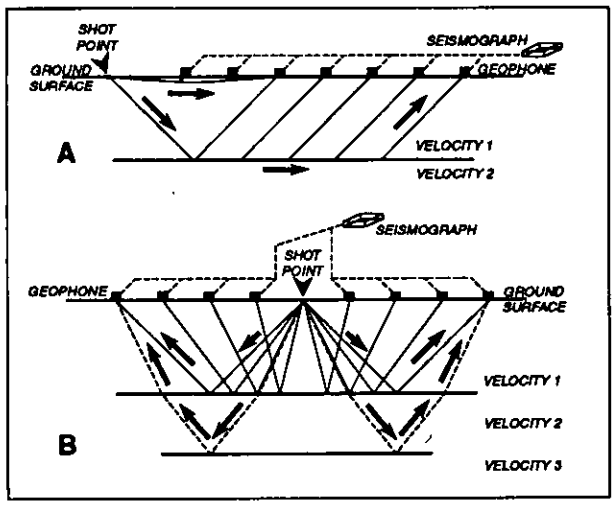

Figure 2. Seismic-wave-propagation schematics showing (A) seismic refraction, and (B) seismic reflection.

At many locations -- mostly in the northern part of the study area -- urbanization precluded line lengths sufficient for refraction investigation. Reflection lines were shot in these areas, generally in small parks or school yards. The data were collected using the wide-angle method as shown by Hunter and others, 1984. The reflection lines in the Hightstown quadrangle showed particularly good results.

All seismic data were collected using a Bison 8012-A, 12-channel engineering seismograph. During the early part of the project, 8-hertz or 100-hertz geophones were used as detectors. Later, Terra Cable ADR 711 accelerometers served this function. Different seismic sources were used depending upon the nature of the background noise. These included a 12-pound sledge hammer, explosives, a 12-gauge "Buffalo Gun," and a vacuum-actuated weightdrop (EG&G Dynasource). A summary of the signal-to-noise capabilities of these sources is given in Miller and others (1986). ADR 711 accelerometers were used for most of the survey because of their ability to amplify with minimal signal distortion, their sensitivity to frequencies greater than 5 hertz, and their suppression of electrical line noise.

The seismic data were field-recorded on cassette tape and subsequently downloaded onto floppy diskettes. The data reduction utilized the computer program HRASSD (Hoffman and Waldner, 1986) to pick time breaks and to calculate layer

velocities. The data were modeled using the SIPT program of Haeni and others (1987).

Electrical Resistivity and Induced Polarization (IP)

Surface electrical resistivity methods were used to delineate hydrogeologic units overlying the bedrock surface. The interpreted resistivity values were used to extend drill hole information laterally and to determine the hydrogeologic structure where no other information was available. Conditions for use of the technique were favorable because differences in resistivity between confining layers and aquifers are substantial. The silts and clays forming confining layers are fairly conductive (resistivity values of 10 to 200 ohm-m). The aquifers, with their sparse clay and fresh water content, have a much higher resistivity (100 to 2,000 ohm-m).

Induced polarization was used in conjunction with resistivity to distinguish between layers with different clay content. The polarizing effect responsible for producing the IP response is related to the ion exchange capacity of the minerals present, especially the clay minerals. Increasing the concentration of clay (up to a critical point) and the presence of clays with high cation exchange capacities produces an increased IP effect (see Keller and Frischknecht, 1966, p. 449); thus, combining the resistivity and IP methods can help to distinguish between massive clays and siltier units.

Resistivity and induced-polarization data interpretation assume that the earth beneath a sounding consists of flat-lying layers, each of which is homogeneous and isotropic with respect to electrical current flow. The dip of the Coastal Plain units is so slight that the assumption of flat-lying layers on the scale of the measurements is appropriate. Electrical homogeneity of the layers is also a valid assumption for these shallow unconsolidated sediments.

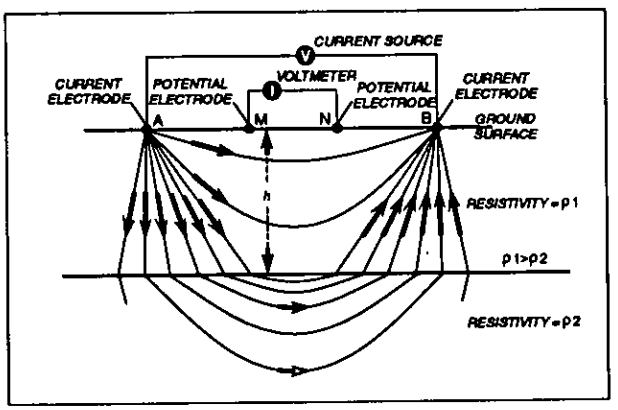

Figure 3. Schlumberger resistivity-array geometry showing lines of current flow in a two-layered earth with higher conductivity in deeper level.

The assumption of electrical isotropy is not entirely valid for clay layers that exhibit depositionally derived or other types of large-scale texture. These textures can produce different electrical properties parallel with or perpendicular to the bedding plane. Interpretational inaccuracy in such cases results in thickness changes in the clay layer rather than the position of its upper boundary.

Eighteen electrical resistivity soundings were collected for this study; at 10 of these sites, IP soundings were also taken (pls. 1, 3). All resistivity and IP data were taken in the Schlumberger array using 10 current electrode spacings per decade (fig. 3). Maximum current electrode spacings ranged from 1,312 to 2,073 feet. All IP soundings, except VES21, were collected with a 20-ms delay after transmitter shut-off and were based on the sum of average voltages at each of 10 consecutive time windows of 20-ms width. VES 21 was collected with a 100-ms delay and gate windows of 100 ms each. In addition, data from 4 Wenner soundings by Dudley (1960) were reinterpreted for inclusion in this report (pl. 3).

A Huntec M4 IP system with a 2.5-kilowatt transmitter-motor generator, steel current electrodes, and copper-copper sulfate porous-pot potential electrodes was used. Resistivity-only data were collected with the ABEM Terrameter SAS battery-powered system using steel electrodes.

Schlumberger resistivity and IP data were reduced to apparent resistivity and chargeability, and plotted versus the half-current electrode separation (AB/2) on a log-log graph. Apparent resistivity calculations were made using the relation:

$$\rho_a = \frac{\pi \cdot MN \cdot V}{I}\left[\left(\frac{AB/2}{MN}\right)^2 - \frac{1}{4}\right]$$

where MN is the distance between potential electrodes, AB is the current electrode separation, V is the voltage observed between potential electrodes, and I is the current transmitted. Apparent chargeability is the instrument output (which consists of the sum of the integrated voltages at the 10 time windows) divided by the received voltage during the current "on" time. The delay time and window width are specified for each sounding in order to relate one sounding to another.

The resistivity and IP data were modeled on a microcomputer using three different algorithms. Resistivity data were modeled using the program SLUMB (Sandberg, 1979). Resistivity-IP data were originally modeled simultaneously using the computer

program CIPINV developed by NJGS. Later revisions were made using EINVRT4 (Sandberg, 1990). Each of the computer programs uses a Marquardt-type nonlinear least squares algorithm in log space for adjusting layer resistivities and thicknesses where the squared error is minimized. The CIPINV and EINVRT4 programs improve resolution of layer thicknesses by taking advantage of the addition of the IP data set to the resistivity information. Appendix 1 contains resistivity- and IP-sounding interpretations showing data fit and layer parameters. The RCSQ parameter shown on these interpretations is the sum of squared residuals normalized by the number of data points minus the number of layered-earth parameters. The L1 norm parameter is the sum of absolute value residuals normalized by the number of data points.

Resistivity and IP data were modeled using a forward routine which calculates the potential due to a layered earth about a single point electrode. The standard Schlumberger approximation, requiring that the potential electrode spacing be much smaller than the current electrode spacing, was not necessary either in the field or in modeling. This algorithm allowed interpretation of the Wenner array data of Dudley (1960) and the so-called "clutches" in Schlumberger array data (in which the current electrode spacing remained constant and the potential electrode spacing increased).

Resistivity and IP modeling used the minimal number of layers needed to fit the data. Attention was given to thin conductive and high resistivity layers as both are known to yield non-unique results due to the inability of the resistivity method to independently resolve both thickness and resistivity. In some cases the incorporation of IP data allowed the thickness-resistivity parameters to decouple and thereby improve resolution.

Gravity

The gravity geophysical method was used to determine bedrock topography and to delineate bedrock contacts beneath the Coastal Plain cover. Geologic conditions were appropriate for the gravity method because there are significant density contrasts among units.

Gravity data were obtained along four traverses (D-D′, E-E′, G-G′, and L-L′). Stations were closely spaced in order to obtain the best possible interpretation of bedrock composition and structure. A LaCoste & Romberg model G gravimeter having an accuracy of 0.01 mGal was used to collect data. Surveying by rod-and-transit provided elevation control except on Line D-D′ where it was obtained from U.S. Geological Survey 7.5-minute topographic quadrangle maps. Horizontal control was determined by surveying tape and 7.5-minute quadrangles.

Gravity data were reduced by microcomputer using a program, developed by Suhas Ghatge (NJGS), which includes corrections for instrument drift, the tidal effects, latitude variation, and both the free-air and Bouguer slab for elevation. The reduced data were interpreted using a computer modeling program developed by NJGS. This is a 2-dimensional Talwani forward algorithm coupled with a nonlinear least squares Marquardt-type inversion algorithm. Regional gravity was inverted to fit a linear gravity gradient.

Assumptions in the interpretation of the gravity data include a linear regional gravity gradient along each profile and homogeneous densities within modeled bodies (prisms). These assumptions are probably valid for the scale of the interpretations presented.

Problems associated with short line lengths in the gravity data are not deemed significant because the modeled regional slope only changes from 0.810 mGal/1,000 ft on line D-D′ in the southwest, to 0.797 mGal/1,000 ft on line E-E′, 0.751 mGal/1,000 ft on line G-G′, and 0.647 mGal/1,000 ft on line L-L′ in the northeast. Regional gradients from a state gravity map (Bonini, 1965) and a newer compilation (D. L. Jagel, formerly of the NJGS, written communication, 1990) are consistent with the values determined in this study. Both compilations show that a linear regional gradient is a good approximation for the relatively short line lengths used.

The densities were assigned using the modeled density contrasts relative to 2.67 g/cm^3. The Cretaceous and younger unconsolidated sediments are assumed to have a density of 1.9 g/cm^3. This is consistent with density values tabulated by Telford and others (1976, p. 25) for wet sands, clays, and gravels; these ranged from 1.7 to 2.5 g/cm^3 and averaged 2.1 g/cm^3.

Triassic sedimentary rocks of the Newark Basin were assigned a density of 2.57 g/cm^3, similar to values of 2.3 to 2.65 g/cm^3 used by Sugarman (1981) and Woollard (1941) for the same units. Kodama (1983) obtained an average density of 2.65 g/cm^3 from six samples of sedimentary rock from the Newark Supergroup. Densities of a wide variety of samples from Telford and others (1976, p. 25) range, for sandstone, from 1.61 to 2.76 g/cm^3, averaging 2.35 g/cm^3 and, for shale, from 1.77 to 3.2 g/cm^3 averaging 2.40 g/cm^3. Densities of diabase and crystalline rock were determined by modeling.

Traverse directions were approximately perpendicular to geologic strike. Gravity was modeled using a 2-dimensional modeling computer program

wherein all gravity prisms extend infinitely along strike (perpendicular to the traverse direction). This is a valid assumption because edge effects caused by distant changes along strike are commonly minor.

Magnetics

The magnetic geophysical method was used in conjunction with gravity interpretation, seismic refraction, and borings to delineate buried contacts between the sedimentary and igneous rocks. To do this, the earth's total magnetic field intensity was measured at discrete points along individual traverses.

The principal assumption used in the magnetic interpretation is that the contribution to the anomaly resulting from susceptibility contrasts is larger than any anomaly contribution due to remanent magnetization. Any errors arising from disregarding remanence are likely to affect modeled magnetic susceptibility rather than orientation of geologic structures. The geologic conditions in the study area were appropriate for use of the magnetic geophysical method because the mafic igneous rocks tend to have a much higher magnetic susceptibility than do the sedimentary rocks.

The most serious limitation of the magnetic method is vulnerability to cultural interference. It is difficult to obtain accurate data in urban areas due to power lines, fences, and other iron or steel objects. Therefore, magnetic data were collected on a limited basis.

Two different proton-precession magnetometers were used: an EG&G Geometrics model G-856 magnetometer (profiles E-E′ and F-F′), and an EDA Omni IV Tie-Line magnetometer (profile B-B′). Both instruments measure the total intensity of the earth's magnetic field in a similar manner and are considered to yield equivalent measurements.

Measurements were made along several traverses of profiles B-B′, E-E′, and F-F′. Station spacings ranged from 25 to 500 feet. Station values consisted of the averages of several readings taken in a closely spaced pattern. Corrections were made for diurnal drift by linear interpolation from base station readings repeated within 2-hour intervals (for profiles E-E′ and F-F′) or from concurrent readings at a base station with a second magnetometer (for profile B-B′). Values were then filtered using a 3-point running average to dampen high frequency noise. Diurnally-corrected magnetic field data for traverses along sections B-B′, E-E′ and F-F′ are shown on plates 2 and 3. For magnetic lines 3, 9, 10, and 11 (pl. 1), these data are found in Appendix 2.

Data modeling was done using a 2.5-dimensional inverse modeling computer program developed for this study. As used here, the 2.5-dimensional model refers to the assumption of a specified strike length of magnetically susceptible bodies and the assumption that the traverse is across the mid-points of the bodies. If the model does not restrict the traverse to mid-points, it is referred to as 3-dimensional. The inversion scheme follows a least squares Marquardt-type procedure.

Magnetic susceptibilities were assigned relative to a background assumed to be zero. A background susceptibility is possible, but this cannot be determined directly from the magnetic data. Magnetic susceptibilities of zero were assigned for Coastal Plain sediments, sedimentary rocks of the Newark Supergroup, and crystalline basement. Susceptibility of the Palisades diabase and an anomalous body within the basement were modeled.

GEOPHYSICAL INTERPRETATIONS

Seismic Refraction and Reflection

In most cases, three-layer models were sufficient to fit the refraction data. Layer one, representing the unsaturated zone, generally had a velocity of 925 to 2,000 ft/s (feet per second). Layer two, saturated, unconsolidated sediments, had velocities ranging from 3,500 to 6,359 ft/s. Layer three is either diabase, at 17,000 ft/s, or sedimentary rocks of the Newark Supergroup, ranging from 7,288 to 15,210 ft/s. Where sedimentary rock of the Newark Supergroup overlies diabase, a four-layer model is necessary.

Other layering was interpreted from the wide-angle reflection data. Within the saturated, unconsolidated sediments, sand layers had velocities of 5,000 to 6,259 ft/s. Clay layers were slightly lower in velocity, ranging from 3,500 to 4,500 ft/s. For comparison, Worzel and Drake (1959) used 5,050 ft/s for unconsolidated sediments overlying Triassic bedrock near Nyack, New York.

Like refraction, seismic reflection shows lower velocities in confining units than in aquifers. For example, SSR40 on cross section K-K′, 2 miles east of Sayreville, shows a thin upper aquifer and confining

unit with a composite velocity of 5,013 ft/s overlying the middle aquifer, which has a slightly higher velocity of 5,477 ft/s. Another example is SSR23, found on cross section B-B'. Here the confining unit has a 4,075-ft/s velocity, compared to the 4,366- and 6,198-ft/s velocities of the upper and middle aquifers.

Seismic velocities that range from 7,288 to 15,210 ft/s were determined for sedimentary rocks of the Newark Supergroup using refraction analysis. This is consistent with an average velocity of 10,000 ft/s derived for the Newark Supergroup beneath the Hudson River at Nyack, New York (Worzel and Drake, 1959). Significant differences in velocity were not discernible among the shale, hornfels, argillite, and sandstone units.

Seismic velocities for the Palisades diabase subcrop ranged from 11,930 to 20,309 ft/s, but were generally determined to be about 17,000 ft/s. Alteration or weathering at the top of the diabase is thought to account for the lower velocities observed on some lines.

Seismic velocities of the crystalline basement rocks ranged from 9,373 to 20,128 ft/s. Like those determined for the diabase, velocities in the crystalline bedrock commonly were close to 17,000 ft/s, substantially higher than those observed in sediments and sedimentary bedrock in this study.

Electrical Resistivity and Induced Polarization (IP)

Resistivity was effective in distinguishing between aquifers and confining units in the Coastal Plain sediments. For example, sounding VES2 on cross section A-A' shows a low resistivity, 114 ohm-m layer, representing the confining unit between the higher resistivity upper and middle aquifers.

Resistivity, together with IP, was effective in distinguishing between silty, clayey confining units and massive clay confining units. To illustrate this, sounding VES 10, on cross section E-E', can be compared with sounding VES 15, on section C-C'. On sounding VES10, a bottom layer with a resistivity of 123 ohm-m and a chargeability of 4.52 ms, contrasts with an overlying aquifer which has a resistivity of 2,300 ohm-m and a chargeability of 2.30 ms. The lower resistivity and higher chargeability of the bottom layer indicates a silty, clayey confining unit. By contrast, the modeled confining unit shown on sounding VES15 is interpreted with more validity as a more massive clay because of its very low resistivity (15 ohm-m) and low chargeability (0.1 ms).

Gravity

Densities of Jurassic diabase obtained by computer modeling of gravity data were 2.98, 3.07, and 2.98 g/cm^3 from cross sections E-E', G-G', and L- L', respectively. Values of 2.7 to 3.1 g/cm^3 were used in modeling by Woollard (1941). Yersak (1977) used 2.95 to 2.97 g/cm^3, and Kodama (1983, p. 154) obtained an average of 2.92 g/cm^3 from measurements on six samples. Densities tabulated for diabase by Telford and others (1976, p. 26) ranged from 2.50 to 3.20 g/cm^3 and averaged 2.91 g/cm^3. The density values obtained by computer modeling in the present study are only slightly higher than those measured by Kodama (1983).

Crystalline rock was assigned a density of 2.80 g/cm^3 in cross section D-D' and 2.90 g/cm^3 in cross section E-E'. Modeling results on cross section G-G' resulted in a value of 2.697 g/cm^3, but the gravity line was not long enough to obtain a very accurate value. Sugarman (1981) used 2.67 g/cm^3 in his modeling; Telford and others (1976, p. 26) shows a range of 2.59 to 3.0 g/cm^3 and an average of 2.80 g/cm^3 for gneisses and a range of 2.39 to 2.9 g/cm^3 and an average of 2.64 g/cm^3 for schists.

Magnetics

Composite magnetic susceptibilities determined for diabase by computer modeling were variable, ranging from 0.00122 cgs in cross section F-F' to 0.0036 cgs in cross section E-E'. Telford and others (1976, p. 121) reported an average susceptibility of 0.0045 cgs for diabase samples. Grant and West (1965, p. 366) reported 0.00259 cgs as the average susceptibility of 19 diabase samples from Minnesota. Kodama (1983, p. 153) showed that the mean susceptibility of the diabase at the basal contact of the Palisades sill was 0.00235 cgs, based upon six samples, and determined to be 0.00202 cgs at the upper contact, based upon five samples. Generally, the composite susceptibilities derived from modeling cannot be directly compared to tabulated values because no account was taken of remanent natural magnetism. However, modeled magnetic susceptibilities are within a factor of two of these tabulated values.

Simultaneous modeling of magnetic and gravity data

Simultaneous modeling of magnetic and gravity data was possible for line E-E'. A fit to both data sets with a single body geometry is thought to decrease the ambiguity of either method taken alone, and hence improves resolution.

GEOLOGIC INTERPRETATION

Bedrock Topography

Topography of the bedrock surface was contoured from (1) well information from Gronberg and others (1989), (2) the seismic work described above, and (3) a compilation of Princeton University thesis work in Runyan, (1961). Plate 1 shows bedrock topography for portions of the study area on the New Brunswick, South Amboy, and Perth Amboy quadrangles; plate 3 shows bedrock topography for portions of the Hightstown and Jamesburg quadrangles.

The interpreted bedrock topography appears as two separate surfaces on cross sections D-D′, E-E′, G-G′, and L-L′. One surface represents the trace of the bedrock surface from plates 2 and 3 (interpretation from well and seismic data), and the other surface represents the model generated from the gravity prism boundaries generated from the modeling of lithologic and density changes within the bedrock. It should be noted that the bedrock surfaces derived from the gravity modeling are less accurate than those generated from the well and seismic data.

Geology and hydrogeology

Bedrock lithologic information in cross sections (pls. 2, 3) is from drillers' logs, seismic velocities, density values from gravity modeling, and magnetic susceptibility values from magnetic modeling. In addition, subdivision of the Potomac-Raritan-Magothy aquifer system is based on (1) lithologic logs, (2) downhole geophysical logs, (3) resistivity/IP modeling, and (4) seismic refraction.

Five groups of geologic units are delineated from these data: 1) unconsolidated sediments of Cretaceous and younger age, 2) Triassic sedimentary rocks of the Newark Basin, 3) Jurassic diabase of the Palisades sill, 4) crystalline basement rocks, and 5) a previously unknown body believed to be part of the crystalline basement but with anomalous magnetic susceptibility and density. The Cretaceous and younger unconsolidated sediments were subdivided into the middle and upper aquifers of the Potomac-Raritan-Magothy aquifer system, the confining layer separating the aquifers, and, on some sections, overlying sediments.

This study constrains and refines the boundaries between the crystalline bedrock and Newark Supergroup sedimentary bedrock and between the Palisades diabase and its enclosing rocks. Other contributions are:

1) Identification of a near pinch-out of the middle aquifer of the Potomac-Raritan-Magothy aquifer system about three miles east-northeast of Sayreville (sections J-J′ and K-K′, pl. 2). This thinning of the aquifer is attributed to bedrock constraints. At this location, the Coastal Plain sediments overlap a bedrock high delineated by seismic refraction lines SSR15, SSR28, and SSR31, and lithologic logs of wells 231025, 231033, 231034, 230842, and 230836. The same thinning of the middle aquifer against bedrock is shown in nearby cross section I-I′ (pl. 2), based on seismic refraction line SSR35 and well 230397 in the Sayreville area. At some locations, the middle aquifer does not rest directly on bedrock, but instead on the Raritan Fire Clay (a saprolite developed on the Passaic Formation).

2) Identification of the termination of the confining unit separating the upper and middle aquifers of the Potomac-Raritan-Magothy aquifer system as the result of a facies change. As shown in cross sections A-A′ and B-B′ (pl. 3), the confining unit changes in an interval extending at least four miles northwestward from Hightstown

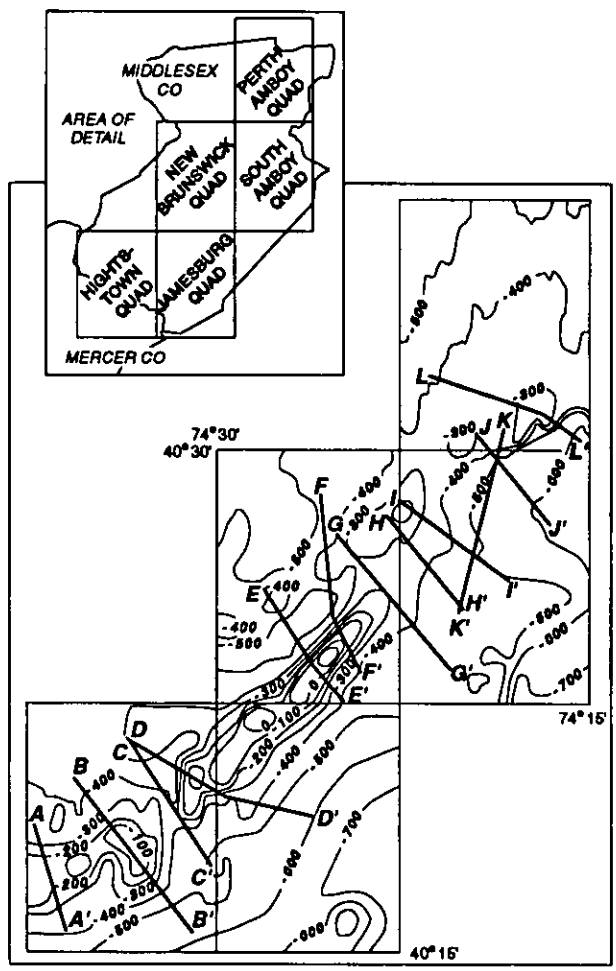

Figure 4. Aeromagnetic map of study area. Contour interval 100 gammas.

from largely clayey, with distinct boundaries downdip, to a sand, which is less distinctly set off from adjacent aquifers updip. On cross section B-B′, well 210085 (near Hightstown) shows distinct upper and middle aquifers separated by a well-defined confining unit, as described in several studies of this area (Pucci and others, 1989; Gronberg, 1991; Pucci and others, 1994). Updip, about two to three miles to the northwest, resistivity soundings VES20 and VES4, extending lithologies from wells 230013, 230778, and 230008, show thickening of the upper aquifer at the expense of the confining unit. Still farther updip, generally higher resistivities (greater than 100 ohm-m), modeled from resistivity soundings VES7, VESD5, and VESD10, indicate that the confining unit in the southeast has passed laterally into a fine sand or sand with thin clay layers. A hydraulic interconnection among all aquifers in this updip part is almost certain.

In an alternative interpretation (Richard Dalton, NJGS, written communication, 1991), the termination of the confining unit is attributed to a post-Cretaceous, sand-and-gravel-filled channel. This channel is recorded in the collection of permanent geologic notes at the New Jersey Geological Survey.

3) Finding of a previously unknown unit believed to be part of the crystalline basement. It was identified using a combination of gravity and magnetic data. This unit appears on the aeromagnetic map (fig. 4) as a highly magnetic body extending southwestward from the New Brunswick quadrangle across the Jamesburg and onto the Hightstown quadrangle. Gravity modeling (cross sections D-D′ and E-E′) gave densities of 2.881 and 2.701 g/cm^3, respectively, for this unit. It should be noted that its density is not well resolved on E-E′, owing to the lack of gravity data on the southeast end of the line. Magnetic modeling from lines E-E′ and F-F′ produced composite susceptibilities of 0.0067, 0.0024, and 0.00287 cgs, respectively. These values are nearly double the modeled diabase susceptibilities on each line and indicate that the rock body is not Mesozoic diabase despite its similarity to the Palisades sill on the aeromagnetic map.

SUMMARY

A variety of surface and borehole geophysical methods has been used in conjunction with lithologic and well drillers' logs to delineate the upper and middle aquifers of the Potomac-Raritan-Magothy aquifer system and underlying bedrock in an area extending from Plainsboro to Perth Amboy in central New Jersey. The surface geophysical methods included electrical resistivity, IP, seismic reflection and refraction, magnetics, and gravity. Twelve interpretive cross sections and two bedrock contour maps show the following:

1. The bedrock surface, along with associated saprolitic clay, defines the lower boundary of the middle aquifer and controls its thickness. A bedrock high in the South Amboy quadrangle, directly south of the Raritan River three miles northeast of Sayreville, correlates with a pinchout of the middle aquifer.

2. A lateral facies change from clay to fine sand terminates the confining unit separating the upper and middle aquifers of the Potomac-Raritan-Magothy aquifer system northeast of Hightstown. This interpretation is based on well logs, electrical resistivity, and IP soundings. In an alternative interpretation, this termination is believed to be due to a previously mapped post-Cretaceous channel.

3. The boundary between the crystalline basement and Newark Supergroup sedimentary bedrock, delineated using gravity modeling, magnetics, and seismic velocities.

4. The subsurface extension of the Palisades sill was delineated more precisely than on previously published maps. This was accomplished by interpreting aeromagnetic information and computer modeling of magnetic and gravity data.

5. A previously unknown body, believed to be a part of the crystalline bedrock with anomalously high density and magnetic susceptibility was delineated using gravity and magnetic modeling.

REFERENCES

Appel, C. A., 1962, Salt-water encroachment into aquifers of the Raritan Formation in the Sayreville Area, Middlesex County, New Jersey: New Jersey Department of Conservation and Economic Development, Division of Water Policy and Supply Special Report 17, 47 p.

Barksdale, H. C., 1937, Water supplies from the no. 1 sand in the vicinity of Parlin, New Jersey: New Jersey State Water Policy Commission Special Report 7, 33 p.

Barksdale, H. C., Johnson, M. E., Schaefer, E. J., Baker, R. C., and DeBuchananne, G. D., 1943, The ground-water supplies of Middlesex County, N. J.: New Jersey State Water Policy Commission Special Report 8, 160 p.

Barton, Cynthia, Vowinkel, E. F., and Nawyn, J. P., 1987, Preliminary assessment of water quality and its relation to hydrogeology and land use: Potomac-Raritan-Magothy Aquifer System, New Jersey: U.S. Geological Survey Water-Resources Investigations Report 87-4023, 79 p.

Bonini, W. E., 1965, Bouguer gravity anomaly map of New Jersey: New Jersey Geological Survey, Geologic Report Series 9, 10 p.

Bonini, W. E., and Woollard, G. P., 1957, Observational accuracy of high-range geodetic type Worden gravimeters: American Geophysical Union Transactions, v. 38, p. 147-155.

Carruthers, J. B., III, 1959, The pre-Cretaceous topography near Princeton-Plainsboro New Jersey: unpublished senior thesis, Princeton University.

Dobrin, M. B., 1976, Introduction to geophysical prospecting: New York, McGraw-Hill, 630 p.

Dudley, W. W., Jr., 1960, Earth-resistivity investigation of the Atlantic Coastal Plain in west-central New Jersey: unpublished B.A. thesis, Princeton University.

Epstein, C. M., 1986, Discovery of the aquifers of the New Jersey Coastal Plain in the nineteenth century, *in* Epstein, C. M., ed., Geological investigations of the Coastal Plain of southern New Jersey, part 2: Hydrogeology of the Coastal Plain: Geological Association of New Jersey, October 1985, Annual Meeting, Pomona, New Jersey, p. 1-21.

Ewing, Maurice, Woollard, G. P., and Vine, A. C., 1939, Geophysical investigations in the emerged and submerged Atlantic Coastal Plain: Geological Society of America Bulletin, v. 50, p. 257-296.

Farlekas, G. M., 1979, Geohydrology and digital-simulation model of the Farrington aquifer in the northern Coastal Plain of New Jersey: U. S. Geological Survey Water-Resources Investigations 79-106, 55 p.

Fiske, R. S., 1955, Plainsboro fault block: a geophysical refutation: unpublished M.S. thesis, Princeton University, 27 p.

Ghatge, S.L., Pasicznyk, D.L., Sandberg, S.K., Hall, D.W., and Groenewold, J.C., 1989, Determination of bedrock topography and geology using various geophysical techniques: New Jersey Geological Survey Technical Memorandum TM 89-2.

Grant, F. S., and West, G. F., 1965, Interpretation theory in applied geophysics: New York, McGraw-Hill, 583 p.

Gronberg, J. M., Birkelo, B. A., and Pucci, A. A., Jr., 1989, Selected borehole geophysical logs and drillers' logs, northern Coastal Plain of New Jersey: U. S. Geological Survey Open-File Report 87-243, 134 p.

Gronberg, J. M., Pucci, A. A., Jr., and Birkelo, B. A., 1991, Hydrogeologic framework of the Potomac-Raritan-Magothy aquifer system, northern Coastal Plain of New Jersey: U.S. Geological Survey Water-Resources Investigations Report 90-4016, 37 p.

Haeni, F. P., Grantham, D. G., and Ellefsen, K., 1987, Microcomputer-based version of SIPT -- a program for the interpretation of seismic-refraction data (text): U. S. Geological Survey Open-File Report 87-103-A, 36 p.

Harriman, D. A., Pope, D. A., and Gordon, A. D., 1989, Water-quality data for the Potomac-Raritan-Magothy aquifer system in the northern Coastal Plain of New Jersey, 1923-86: New Jersey Geological Survey Report GSR 19, 94 p.

Hickok, E. A., 1954, Ground water geology of the Princeton area: unpublished M.S. thesis, Princeton University.

Hoffman, J. L., and Waldner, J. S., 1986, High resolution analysis of shallow seismic data: HRASSD 2.0: New Jersey Geological Survey Open-File Report OFR 86-1, 74 p.

Hunter, J. A., Pullan, S. E., Burns, R. A., Gagne, R. M., and Good, R. L., 1984, Shallow seismic reflection mapping of the overburden-bedrock interface with the engineering seismograph -- some simple techniques: Geophysics, v. 49, no. 8, p. 1381-1385.

Keller, G. V., and Frischknecht, F. C., 1966, Electrical methods in geophysical prospecting: New York, Pergamon Press, 517 p.

Knapp, G. N., 1904, Underground waters of New Jersey, *in* New Jersey Geological Survey Annual Report of the State Geologist, 1903, p. 73-93.

Kodama, K. P., 1983, Magnetic and gravity evidence for a subsurface connection between the Palisades sill and the Ladentown basalts: Geological Society of America Bulletin, v. 94, p. 151-158.

Kummel, H. B., and Poland, H. M., 1910, Records of wells in New Jersey, 1905-1909, *in* New Jersey Geological Survey Annual Report of the State Geologist, 1909, p. 69-100.

Leahy, P. P., Paulachok, G. N., Navoy, A. S., and Pucci, A. A., Jr., 1987, Plan of study for the New Jersey bond issue ground-water supply investigations: New Jersey Geological Survey Open-File Report 87-1, 53 p.

LKB Resources, Inc., 1980, Magnetic contour maps: *in* NURE Aerial Gamma-Ray and Magnetic Reconnaissance Survey - Thorpe Area - Newark NK18-11 Quadrangle, Volume II, prepared for the Department of Energy, Grand Junction, Colorado.

Meier, D. R., 1949, Geophysical investigations in the Trenton-Old Bridge area: unpublished M.S. thesis, Princeton University, 48 p.

Miller, R. D., Pullan, S. E., Waldner, J. S., and Haeni, F. P., 1986, Field comparison of shallow seismic sources: Geophysics, v. 51, no. 11, p. 2067-2092.

New Jersey Geological Survey, 1990, Generalized stratigraphic table for New Jersey: Information Circular 1, 1 sheet.

Owens, J. P., and Gohn, G. S., 1985, Depositional history of the Cretaceous Series in the U.S. Atlantic Coastal Plain: stratigraphy, paleoenvironments, and tectonic controls of sedimentation, *in* C. W. Poag, ed., Geology of the continental margins: New York, Van Nostrand-Wiley, p. 25-86.

Owens, J. P., and Sohl, N. F., 1969, Shelf and deltaic paleoenvironments in the Cretaceous-Tertiary formations of the New Jersey Coastal Plain, *in* Subitzky, Seymour, ed., Geology of selected areas in New Jersey and eastern Pennsylvania and guidebook of excursions: New Brunswick, New Jersey, Rutgers University Press, p. 235-278.

Owens, J. P., Sohl, N. F., and Minard, J. P., 1977, A field guide to Cretaceous and lower Tertiary beds of the Raritan and Salisbury embayments, New Jersey, Delaware, and Maryland: Washington D. C., American Association of Petroleum Geologists-Society of Economic Paleontologists and Mineralogists, 113 p.

Pucci, A. A., Jr., Gronberg, J. M., and Pope, D. A., 1989, Hydraulic properties of the middle and upper aquifers of the Potomac-Raritan-Magothy aquifer system in the northern Coastal Plain of New Jersey: New Jersey Geological Survey Report GSR 18, 74 p.

Pucci, A. A., Jr., Pope, D. A., Gronberg, J. M., 1994, Hydrogeology, simulation of regional ground-water flow, and saltwater intrusion, Potomac-Raritan-Magothy aquifer system, northern Coastal Plain of New Jersey: New Jersey Geological Survey Geological Survey Report GSR 36, 209 p.

Runyan, D. R., 1961, Bedrock topography of the Kingston-Plainsboro-Monmouth Junction area: unpublished B.S. thesis, Princeton University, 51 p.

Sandberg, S. K., 1979, Documentation and analysis of the Schlumberger interactive 1-D inversion program SLUMB: University of Utah Department of Geology and Geophysics report DOE/ET/27002-2, 84 p.

_____,1990, Microcomputer software for individual or simultaneous inverse modeling of transient electromagnetic, resistivity, and induced polarization soundings: New Jersey Geological Survey Open-File Report OFR 90-1, 160 p., 2 diskettes.

Sandberg, S. K., and Hall, D. W., 1990, Geophysical investigation of an unconsolidated coastal plain aquifer system and the underlying bedrock geology in central New Jersey, *in* Ward, S. H., ed., Geotechnical and Environmental Geophysics, v. 2: Environmental and Groundwater: Investigations in Geophysics No. 5, Society of Exploration Geophysicists, Tulsa, Oklahoma, p. 311-320.

Schaefer, F. L., 1983, Distribution of chloride concentrations in the principal aquifers of the New Jersey Coastal Plain, 1977-81: U.S. Geological Survey Water-Resources Investigations Report 83-4061, 56 p.

Sugarman, P. J., 1981, The geological interpretation of gravity anomalies in the vicinity of Raritan Bay,

New Jersey and New York: University of Delaware unpublished M.S. thesis, 135 p.

Telford, W. M., Geldart, L. P., Sheriff, R. E., and Keys, D. A., 1976, Applied Geophysics: Cambridge, Cambridge University Press, 860 p.

Varrin, R. D., 1957, A pre-Cretaceous channel in the Plainsboro N.J. area as determined by seismic refraction measurements: unpublished M.S. thesis, Princeton University, 35 p.

Woollard, G. P., 1941, Geophysical methods of exploration and their application to geological problems in New Jersey: New Jersey Department of Conservation and Development Bulletin 54, 89 p.

Woolman, Lewis, 1889 - 1902, Report on artesian wells, *published annually in* Annual report of the State Geologist: New Jersey Geological Survey, Trenton, New Jersey.

Worzel, J. L., and Drake, C. L., 1959, Structure section across the Hudson River at Nyack, N. Y., from seismic observations: N. Y. Academy of Sciences, Annals, v. 80, p. 1092-1105.

Yahn, W. J., 1945, The Millstone River problem: unpublished B.S. thesis, Princeton University, 30 p.

Yersak, R. E., 1977, Gravity study of Staten Island and vicinity: unpublished M.S. thesis, Rutgers University, 48 p.

Zapecza, O.S., 1989, Hydrogeologic framework of the New Jersey Coastal Plain: U.S. Geological Survey Professional Paper 1404-B, 49 p.

Table 3. Seismic line locations and field parameters (--, seismic line not used in cross section)

Line number	Location Lat./Long. (deg., min., sec.)	Cross Section(s) / plate number	Geophone spacing (feet)	Shot point locations (ft. from geophone G1)
SSR1	40 17 04 74 36 24	A-A' 3	50	1 -550 2 -225 3 25 4 275 5 525 6 775 7 1100
SSR2	40 16 21 74 36 17	A-A' 3	50	1 -550 2 25 3 525 4 1100
SSR3	40 19 04 74 33 44	-- 3	50	1 -550 2 -275 3 25 4 275 5 525 6 825 7 1100
SSR5	40 19 38 74 35 52	B-B' 3	20	1 -100 2 -50
SSR6	40 19 38 74 35 53	-- 3	50	1 -275 2 25 3 275 4 525 5 825
SSR7	40 19 04 74 34 57	B-B' 3	50	1 -550 2 -275 3 25 4 275 5 525 6 825 7 1084
SSR8	40 16 53 74 32 22	B-B' 3	50	1 -275 2 25 3 275 4 525 5 825 6 1100
SSR8A	40 16 53 74 32 22	B-B' 3	20	1 370 2 420
SSR9A	40 24 03 74 26 18	E-E' 2	50	1 -550 2 -275 3 25 4 525 5 825 6 1100
SSR10	40 23 06 74 25 55	E-E' 2	50	1 -275 2 25 3 275 4 525 5 825 6 1100
SSR12	40 26 34 74 24 44	G-G' 2	20	1 -300 2 -150 3 10 4 110 5 210 6 370 7 520
SSR13	40 28 00 74 22 15	-- 1	20	1 -200 2 -100 3 10 4 110 5 210 6 310
SSR15	40 28 48 74 18 44	K-K' 2	20	1 -250 2 -100 3 10 4 110 5 210 6 310 7 420
SSR16	40 30 12 74 19 20	J-J' 2	20	1 -200 2 -100 3 10 4 110 5 210 6 310 7 410
SSR17	40 29 18 74 21 06	-- 1	20	1 -200 2 -100 3 10 4 110 5 210 6 310
SSR20	40 29 18 74 21 06	E-E' 2	20	1. -300 2 -150 3 10 4 110 5 210 6 370 7 520
SSR21	40 20 22 74 32 30	C-C' 3	50	1 -550 2 -275 3 25 4 275 5 525 6 825
SSR22	40 21 13 74 33 15	C-C' D-D' 3	50	1 -275 2 25 3 275 4 525
SSR23	40 17 36 74 32 45	B-B' 3	20	1 -90 2 -50 3 446

Table 3 -- continued. Seismic line locations and field parameters

Line number	Location Lat./Long. (deg., min., sec.)	Cross Section(s) plate number	Geo-phone spacing (feet)	Shot point locations (ft. from geo-phone G1)
SSR24	40 18 47 74 30 20	C-C' 3	20	1 -100 2 -50
SSR25	40 25 17 74 26 50	E-E' 2	50	1 -500 2 -275 3 25 4 525 5 825
SSR26A	40 20 02 74 36 19	B-B' 3	20	1 -60
SSR27	40 27 45 74 21 12	I-I' 2	50	1 -150 2 25 3 525 4 700
SSR28	40 29 13 74 18 21	J-J' K-K' 2	50	1 -150 2 25 3 525 4 700
SSR29	40 19 25 74 35 06	B-B' 3	50	1 -275 2 25 3 525 4 825
SSR30	40 26 08 74 21 08	H-H' 2	50	1 -550 2 -350 3 25 4 525 5 1100
SSR31	40 29 20 74 18 21	J-J' K-K' 2	50	1 -550 2 25 3 525 4 1100
SSR32	40 25 53 74 19 59	K-K' 2	50	1 -550 2 25 3 525 4 1100
SSR33	40 25 50 74 20 35	H-H' 2	50	1 -450 2 25 3 525 4 1000
SSR34	40 27 10 74 21 33	H-H' 2	50	1 -330 2 86 3 525 4 850
SSR35	40 28 13 74 21 45	I-I' 2	50	1 -300 2 25 3 525 4 750
SSR36	40 18 13 74 37 22	A-A' 3	50	1 -200 2 25 3 275 4 525 5 750
SSR38	40 19 53 74 31 43	C-C' 3	50	1 -140 2 275 3 690
SSR39	40 20 42 74 31 36	D-D' 3	50	1 -150 2 275 3 700
SSR40	40 27 51 74 19 10	K-K' 2	20	1 420
SSR41	40 26 42 74 22 02	H-H' 2	20	1 -400 2 -200 3 110 4 420 5 520 6 620 7 720
SSR43A	40 26 03 74 23 40	G-G' 2	50	1 -300 2 -200 3 275 4 755 5 850 6 950
SSR45	40 26 13 74 25 43	F-F' 2	6	1 -100
SSR47	40 31 43 74 17 00	L-L' 2	20	1 -200 2 10 3 206 4 320
SSR48	40 31 20 74 17 30	L-L' 2	6	1 -100

Table 4. Interpreted depths and velocities to seismic interfaces

Line number	Elevation (ft.)	Layer		Depth (feet to top, under geophone)		
		no.	velocity (ft./sec)	G1	G6	G12
SSR1	100	1	1775			
		2	5429	35	30	29
		3	17363	155	168	152
SSR2	90	1	3022			
		2	5535	39	28	16
		3	17293	161	185	195
SSR3	90	1	1621			
		2	5235	16	20	19
		3	17717	183	167	159
SSR5 (reflection)	75	1	4334			
		2	8801	97		
		3		470		
SSR6	70	1	1491			
		2	3624	10	20	2
		3	11093	91	76	86
SSR7	80	1	1681			
		2	5064	19	23	24
		3	17714	214	188	184
SSR8	100	1	1567			
		2	5674	20	19	17
SSR8A (reflection)	100	1	4471			
		2	8435	192		
		3	7632	252		
		4	14623	360		
SSR9A	120	1	1592			
		2	5420	41	43	50
		3	14974	241	252	227
SSR10	58	1	1646			
		2	5627	28	21	17
SSR12	100	1	1310			
		2	5399	11	12	16
		3	11930	138	133	131
SSR13	5	1	1140			
		2	5855	21	19	19
		3	14547	91	93	94
SSR15	50	1	3132.			
		2	5698	19	20	22
		3	17119	103	142	160
SSR16	5	1	1425			
		2	5521	18	21	14
		3	15210	71	65	77
SSR17	5	1	1639			
		2	7816	10	12	16
		3	12545	68	38	16
SSR20	110	1	1420			
		2	5397	11	10	5
		3	11534	44	58	71
		4	20309	113	126	155
SSR21	100	1	2058			
		2	5303	27	19	21
		3	11007	164	174	177
SSR22	100	1	1995			
		2	6259	26	28	27
		3	16452	120	172	188
SSR23 (reflection)	85	1	4366			
		2	4074	120		
		3	6198	191		
		4		293		
SSR24 (reflection)	90	1	5508			
		2	6315	95		
		3	6722	119		
		4	7842	142		
		5	4874	185		
		6	6499	248		
		7		338		
SSR25	90	1	4381			
		2	19995	82	85	88
SSR26A (reflection, on outcrop)	65	1	10153	outcrop		

Table 4 -- continued. Interpreted depths and velocities to seismic interfaces

Line number	Elevation (ft.)	Layer		Depth (feet to top, under geophone)		
		no.	velocity (ft./sec)	G1	G6	G12
SSR27	70	1	3867			
		2	17375	153	159	178
SSR28	30	1	3429			
		2	17090	104	97	78
SSR29	80	1	1458			
		2	4641	20	30	28
		3	17184	118	122	122
SSR30	10	1	925			
		2	5527	13	13	12
		3	9373	298	255	232
SSR31	100	1	1215			
		2	5529	12	14	4
		3	12704	189	191	216
SSR32	20	1	3375			
		2	5554	85	90	68
		3	16665	313	325	329
SSR33	10	1	1513			
		2	5492	16	15	15
		3	12037	242	223	175
SSR34	50	1	3570			
		2	5181	40	39	3
		3	11760	207	166	164
SSR35	10	1	2437			
		2	14311	57	54	53
SSR36	100	1	1987			
		2	16054	27	25	21
SSR38	90	1	4648			
		2	14706	177	193	206
SSR39	100	1	3771			
		2	20128	137	141	152
SSR40	35	1	5013			
(reflection)		2	5477	119		
		3		197		
SSR41	10	1	1923			
		2	5400	8	8	7
		3	13604	171	166	157
SSR43A	120	1	1950			
		2	5520	43	36	35
		3	11136	173	180	175
SSR45	120	1	3302			
(reflection)		2		101		
SSR47	120	1	2182			
		2	4830	15	24	19
		3	7288	90	87	70
SSR48	90	1	1782			
(reflection)		2	2174	25		
		3		52		

Table 5. Electrical resistivity and induced polarization (IP) sounding locations, elevations, and data-fit errors (--, sounding location not used in cross section)

Line number	Location Lat./Long. (deg., min, sec.)	Cross section	Elevation (ft.)	Data fit (RCSQ)
VES1	40 17 04 74 36 24	A-A '	100	0.00009 (res)
VES2	40 16 22 74 36 18	A-A '	90	0.00047 (res)
VES3	40 19 06 74 33 44	--	85	0.00081 (res)
VES4	40 17 49 74 33 16	B-B '	90	0.00066 (res)
VES5	40 19 38 74 35 52	B-B '	60	0.00029 (res)
VES6	40 19 32 74 35 53	--	80	0.00094 (res)
VES7	40 19 04 74 34 57	B-B '	85	0.00011 (res)
VES8	40 16 53 74 32 22	B-B '	100	0.00026 (res)
VES10	40 24 05 74 26 11	E-E '	120	0.00077 (res) 0.02045 (IP)
VES11	40 25 26 74 27 35	E-E '	100	0.00376 (res) 0.06641 (IP)
VES12	40 26 16 74 27 14	--	90	0.00049 (res) 0.08443 (IP)
VES13	40 30 36 74 19 03	J-J '	10	0.00067 (res) 0.10357 (IP)
VES16	40 18 52 74 31 48	C-C '	95	0.00071 (res) 0.01687 (IP)
VES17	40 17 07 74 36 30	A-A '	100	0.00047 (res) 0.01407 (IP)
VES18	40 18 35 74 35 30	--	85	0.00097 (res) 0.07748 (IP)
VES20	40 18 15 74 34 18	B-B '	80	0.00010 (res) 0.04021 (IP)
VES21	40 27 54 74 19 22	K-K '	50	0.00049 (res) 0.05040 (IP)
VESD3	40 17 40 74 34 50	--	90	0.00018 (res)
VESD5	40 18 50 74 34 28	B-B '	80	0.00018 (res)
VESD10	40 18 37 74 34 30	B-B '	80	0.00016 (res)
VESD14	40 16 04 74 35 58	A-A '	80	0.00024 (res)

Table 6. U. S. Geological Survey Ground Water Site Inventory (GWSI) numbers of wells used in this report, and corresponding New Jersey Bureau of Water Allocation permit numbers (--, no corresponding number)

GWSI number	Permit number	GWSI number	Permit number	GWSI number	Permit number	GWSI number	Permit number
210001	--	230133	--	230410	--	230622	48-00093
210013	28-06864	230135	29-04998	230411	46-00144	230623	48-00090
210017	28-01274	230146	--	230421	--	230624	48-00091
210019	28-05897	230147	--	230424	--	230625	48-00092
210022	28-05440	230154	--	230425	--	230626	48-00095
210024	28-05053	230156	--	230430	--		
210025	--	230170	--	230438	28-09722	230762	28-13649
210081	--	230171	--	230439	--	230764	29-10831
210084	--	230172	--	230442	28-07828	230766	28-08774
210085	28-09493	230176	--	230443	--	230769	28-12772
210086	28-09494	230179	--	230445	--	230770	28-12877
		230191	--	230446	--	230772	28-01994
210130	28-03045	230194	--	230447	28-02172	230774	28-12288
210143	--	230197	--	230448	28-02173	230778	28-13514
210145	--			230453	--	230779	28-08750
210152	--	230201	--	230462	--	230781	28-11788
		230202	--	230479	--	230783	29-12817
210241	28-15613	230206	--			230784	28-13023
		230219	--	230501	--	230787	23-12434
230008	28-01176	230230	--	230504	--	230790	28-15614
230010	NA	230231	--	230505	--	230791	28-15615
230011	28-02321	230232	28-04106	230506	--		
230012	--	230238	28-05123	230510	28-10269	230816	--
230013	--	230241	--	230522	--	230817	--
230014	--	230255	--	230527	28-00222	230818	--
230017	--	230260	--	230538	--	230827	--
230020	28-06292	230265	--	230541	--	230836	--
230025	28-05007	230273	--	230551	28-11524	230842	--
230030	--	230291	--	230553	--	230848	--
230034	--	230292		230573	26-03264	230850	--
230039	--	230293	--	230574	26-04398	230859	--
230040	--	230297	--	230575	26-04635		
230042	--			230576	26-04710	230925	--
230044	--	230300	--	230577	26-05321	230944	--
230046	--	230302	--	230578	26-05324	230963	--
230047	--	230315	--	230580	28-01524	230969	--
230048	--	230319	--	230581	28-08423	230971	--
230050	28-04657	230322	--	230582	28-10495	230995	--
230057	--	230327	--	230584	28-10626		
230058	--	230328	--	230585	28-11899	231000	--
230059	--	230330	--	230587	28-12534	231002	--
230061	--	230332	28-03140	230590	29-01391	231004	--
230065	--	230352	--	230591	29-01390	231005	--
230066	--	230365	--	230592	29-01593	231007	--
230067	28-03548	230369	--	230595	29-11118	231011	--
230068	--	230370	--	230598	28-08814	231012	--
230071	--	230371	--			231013	--
230072	--	230376	--	230600	49-00027	231016	--
230073	--	230377	--	230601	49-00026	231017	--
230075	--	230379	--	230603	49-00025	231021	--
230077	--	230380	--	230608	48-00077	231024	--
230079	--	230384	--	230609	48-00078	231025	--
230082	--	230386	--	230610	48-00079	231027	--
230094	--	230390	--	230611	48-00080	231029	--
230097	--	230391	--	230612	48-00081	231031	--
		230395	--	230613	48-00082	231033	--
230100	28-01612	230396	--	230614	48-00083	231034	--
230101	--	230397	--	230615	48-00084	231037	26-00125
230107	--	230398	--	230616	48-00085	231038	26-00126
230114	--	230399	--	230617	48-00086	231039	26-00123
230119	--			230618	48-00087	231058	28-17742-5
230127	--	230404	--	230619	48-00088		
230131	--	230408	--	230620	48-00089	--	28-13082
230132	--	230409	--	230621	48-00094		

Table 7. Principal facts of gravity stations

[density = 2.670 g/cm3; Theoretical Sea-Level Gravity, TSLGV, based on 1930 International Gravity Formula; principal gravity base station at Princeton University (Bonini and Woollard, 1957); observed gravity = 980177.6 mGal; meter = Lacoste-Romberg #G77]

Station number	Location (lat./long., deg, decimal min.)	Elevation	Gravity (mGal)		
			Observed	Theoretical Sea-level	Simple Bouguer Anomaly
Cross-section D-D'					
1	40 21.17 74 33.38	102.0	980194.583	980211.857	-11.157
2	40 21.10 74 33.05	101.0	980195.870	980211.753	-9.827
3	40 21.02 74 32.65	103.0	980196.835	980211.634	-8.623
4	40 20.85 74 32.10	103.0	980198.749	980211.382	-6.456
5	40 20.70 74 31.63	98.0	980200.553	980211.160	-4.730
6	40 20.60 74 31.17	96.0	980202.955	980211.011	-2.300
7	40 20.30 74 30.15	104.0	980207.253	980210.566	2.924
8	40 19.93 74 29.50	108.0	980209.562	980210.017	6.021
9	40 19.62 74 29.30	110.0	980210.058	980209.557	7.097
10	40 19.60 74 28.92	110.0	980210.385	980209.528	7.453
11	40 19.45 74 28.25	124.0	980210.612	980209.305	8.743
12	40 19.25 74 27.15	152.0	980209.928	980209.008	10.034
13	40 19.00 74 26.32	157.0	980211.330	980208.638	12.107
14	40 20.35 74 30.53	106.0	980205.843	980210.640	1.559
15	40 19.52 74 28.58	116.0	980211.354	980209.409	8.901
16	40 19.42 74 27.93	130.0	980209.604	980209.261	8.139
17	40 19.30 74 27.62	142.0	980209.488	980209.083	8.920
18	40 19.18 74 26.70	156.0	980211.327	980208.905	11.777
Cross-section E-E'					
1	40 22.93 74 25.37	46.0	980220.201	980214.463	8.497
2	40 23.01 74 25.45	40.0	980219.957	980214.587	7.769
3	40 23.08 74 25.55	45.0	980219.055	980214.694	7.059
4	40 23.14 74 25.68	48.0	980218.020	980214.786	6.112
5	40 23.19 74 25.80	70.0	980215.817	980214.848	5.166
6	40 23.27 74 25.90	90.0	980213.347	980214.975	3.769

Table 7 -- continued. Principal facts of gravity stations

[density = 2.670 g/cm3; Theoretical Sea-Level Gravity, TSLGV, based on 1930 International Gravity Formula; principal gravity base station at Princeton University (Bonini and Woollard, 1957); observed gravity = 980177.6 mGal; meter = Lacoste-Romberg #G77]

Station number	Location (lat./long., deg, decimal min.)	Elevation	Gravity (mGal)		
			Observed	Theoretical Sea-level	Simple Bouguer Anomaly
Cross-section E-E′ --continued					
7	40 23.34 74 25.99	108.0	980211.395	980215.080	2.792
8	40 23.42 74 26.09	118.0	980210.153	980215.196	2.033
9	40 23.51 74 26.20	145.0	980207.216	980215.322	.589
10	40 23.59 74 26.28	140.0	980207.121	980215.447	.070
11	40 23.67 74 26.34	125.0	980207.487	980215.573	-.590
12	40 23.78 74 26.41	115.0	980207.626	980215.727	-1.205
13	40 23.88 74 26.46	100.0	980207.794	980215.881	-2.091
14	40 23.97 74 26.53	108.0	980207.519	980216.016	-2.021
15	40 24.06 74 26.60	105.0	980206.658	980216.147	-3.193
16	40 24.17 74 26.67	100.0	980206.641	980216.315	-3.678
17	40 24.27 74 26.74	95.0	980206.888	980216.460	-3.876
18	40 24.23 74 26.80	85.0	980206.886	980216.402	-4.419
19	40 24.47 74 26.85	90.0	980205.860	980216.759	-5.501
20	40 24.62 74 26.89	105.0	980204.898	980216.981	-5.786
21	40 24.65 74 27.02	105.0	980205.045	980217.020	-5.679
22	40 24.68 74 27.16	98.0	980205.298	980217.058	-5.884
23	40 24.70 74 27.31	88.0	980206.231	980217.097	-5.589
24	40 24.78 74 27.40	85.0	980207.494	980217.213	-4.621
25	40 24.82 74 27.53	92.0	980207.138	980217.266	-4.612
26	40 24.84 74 27.67	95.0	980207.119	980217.309	-4.494
27	40 24.88 74 27.81	92.0	980206.971	980217.363	-4.875
28	40 24.91 74 27.94	90.0	980206.897	980217.406	-5.112
29	40 24.97 74 28.08	85.0	980207.328	980217.502	-5.077
30	40 25.04 74 28.20	85.0	980207.077	980217.599	-5.425
31	40 25.10 74 28.31	82.0	980206.203	980217.695	-6.575
32	40 25.17 74 28.41	90.0	980205.974	980217.792	-6.421

Table 7 -- continued. Principal facts of gravity stations

[density = 2.670 g/cm3; Theoretical Sea-Level Gravity, TSLGV, based on 1930 International Gravity Formula; principal gravity base station at Princeton University (Bonini and Woollard, 1957); observed gravity = 980177.6 mGal; meter = Lacoste-Romberg #G77]

Station number	Location (lat./long., deg, decimal min.)	Elevation	Gravity (mGal)		
			Observed	Theoretical Sea-level	Simple Bouguer Anomaly
Cross-section E-E′ --continued					
33	40 25.25 74 28.53	93.0	980205.196	980217.907	-7.135
34	40 25.22 74 28.59	67.0	980206.375	980217.869	-7.476
35	40 25.44 74 28.63	55.0	980207.590	980218.197	-7.309
36	40 25.48 74 28.77	60.0	980207.138	980218.255	-7.519
Cross-section G-G′					
1	40 24.85 74 20.024	18.36	980225.094	980217.318	8.877
2	40 24.99 74 22.109	54.22	980222.165	980217.521	7.895
3	40 25.12 74 22.211	124.55	980217.084	980217.714	6.839
4	40 25.25 74 22.33	163.88	980214.251	980217.906	6.172
5	40 25.39 74 22.466	160.24	980214.213	980218.118	5.703
6	40 25.56 74 22.755	159.37	980213.579	980218.367	4.768
7	40 25.70 74 22.755	158.97	980212.779	980218.579	3.733
8	40 25.86 74 22.891	152.48	980212.492	980218.810	2.825
9	40 25.98 74 23.01	154.80	980211.618	980218.992	1.908
10	40 26.11 74 23.146	142.52	980211.972	980219.194	1.323
11	40 26.26 74 23.282	140.61	980211.287	980219.406	.313
12	40 26.37 74 23.384	127.34	980211.836	980219.570	-.098
13	40 26.52 74 23.52	113.90	980213.077	980219.790	.117
14	40 26.65 74 23.623	109.81	980213.594	980219.983	.196
15	40 26.76 74 23.708	110.29	980213.422	980220.146	-.110
16	40 26.90 74 23.742	96.90	980214.531	980220.358	-.017
17	40 26.99 74 23.869	93.45	980214.849	980220.492	-.040
18	40 27.13 74 23.946	94.99	980214.559	980220.704	-.449
19	40 27.29 74 24.031	88.14	980214.693	980220.934	-.956
20	40 27.44 74 24.099	88.09	980214.363	980221.155	-1.510

Table 7 -- continued. Principal facts of gravity stations

[density = 2.670 g/cm3; Theoretical Sea-Level Gravity, TSLGV, based on 1930 International Gravity Formula; principal gravity base station at Princeton University (Bonini and Woollard, 1957); observed gravity = 980177.6 mGal; meter = Lacoste-Romberg #G77]

Station number	Location (lat./long., deg, decimal min.)	Elevation	Gravity (mGal)		
			Observed	Theoretical Sea-level	Simple Bouguer Anomaly
Cross-section G-G ' --continued					
21	40 27.64 74 24.235	105.14	980213.208	980221.464	-1.952
22	40 27.80 74 24.252	92.78	980214.058	980221.694	-2.073
23	40 27.94 74 24.379	84.34	980214.308	980221.905	-2.540
24	40 28.04 74 24.446	72.94	980214.578	980222.060	-3.108
25	40 28.21 74 24.541	74.92	980213.972	980222.309	-3.84
Cross-section L-L '					
1	40 30.53 74 15.707	7.8	980234.051	980225.745	8.775
2	40 30.65 74 16.138	42.6	980230.713	980225.926	7.338
3	40 30.83 74 16.414	56.6	980229.158	980226.195	6.360
4	40 30.91 74 16.56	64.7	980228.825	980226.314	6.394
5	40 31.02 74 16.724	76.9	980228.416	980226.478	6.549
6	40 31.17 74 16.983	104.3	980226.623	980226.700	6.174
7	40 31.30 74 17.241	82.2	980228.028	980226.893	6.070
8	40 31.43 74 17.793	78.6	980226.893	980227.086	4.523
9	40 31.57 74 18.376	126.8	980221.593	980227.297	1.898
10	40 31.74 74 19.043	116.2	980220.643	980227.548	0.059
11	40 31.81 74 19.303	111.7	980220.258	980227.644	-.688
12	40 31.86 74 19.634	109.4	980219.802	980227.732	-1.370
13	40 31.92 74 19.813	111.1	980218.872	980227.819	-2.288
14	40 32.03 74 20.068	107.7	980218.402	980227.972	-3.111
15	40 32.10 74 20.34	105.8	980217.678	980228.089	-4.069
16	40 32.17 74 20.663	102.5	980216.925	980228.185	-5.116
17	40 32.21 74 21.191	94.8	980216.275	980228.252	-6.291

APPENDIXES 1 - 2

Resistivity and Induced Polarization (IP) sounding interpretations showing data fit and layer parameters, and diurnally corrected magnetic data.

APPENDIX 1

Resistivity and induced polarization (IP) sounding interpretations showing data-fit and layer parameters.

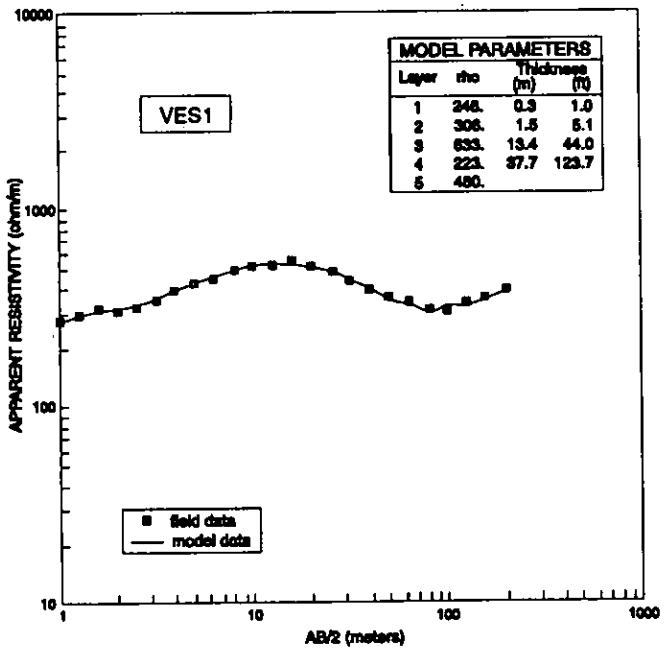

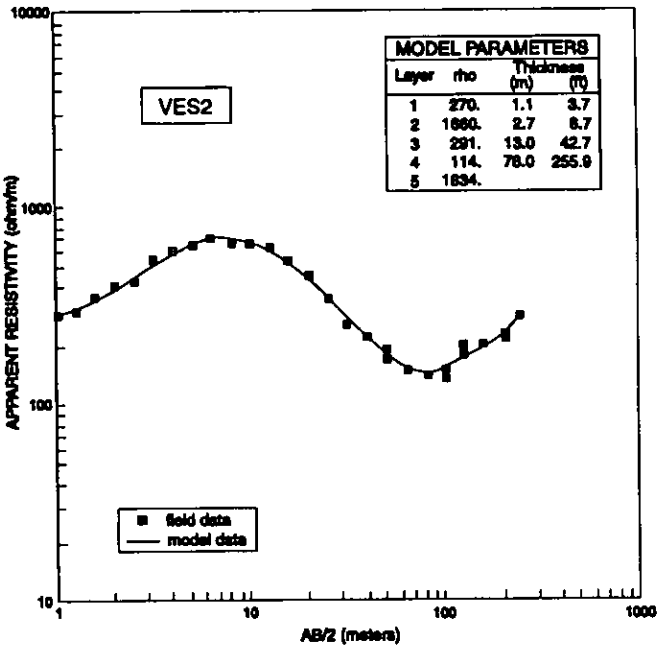

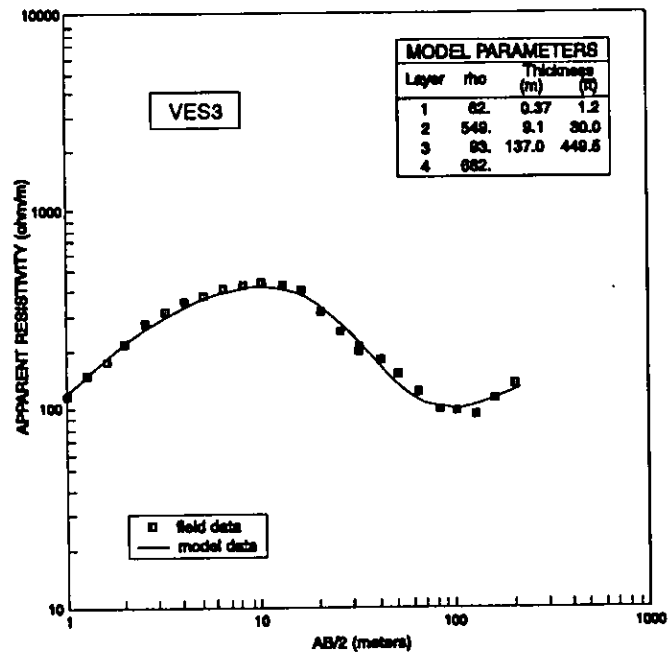

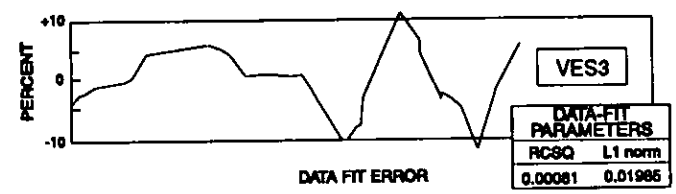

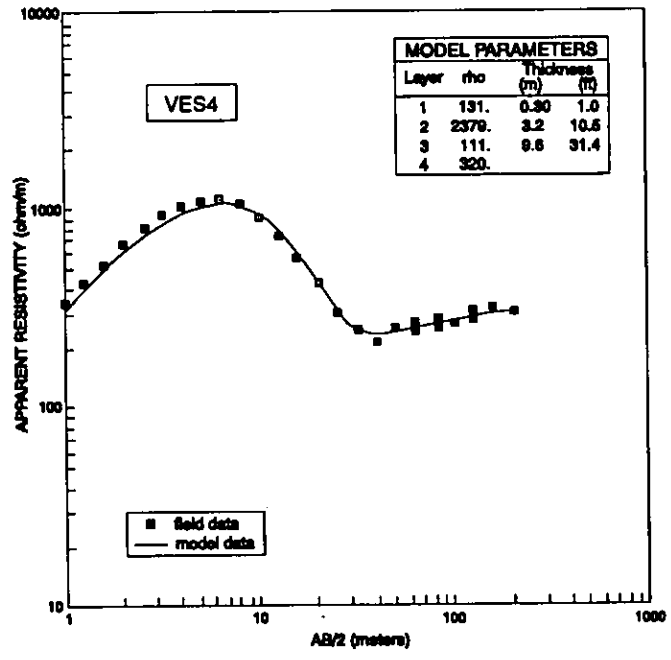

APPENDIX 1-- continued

Resistivity and induced polarization (IP) sounding interpretations showing data-fit and layer parameters.

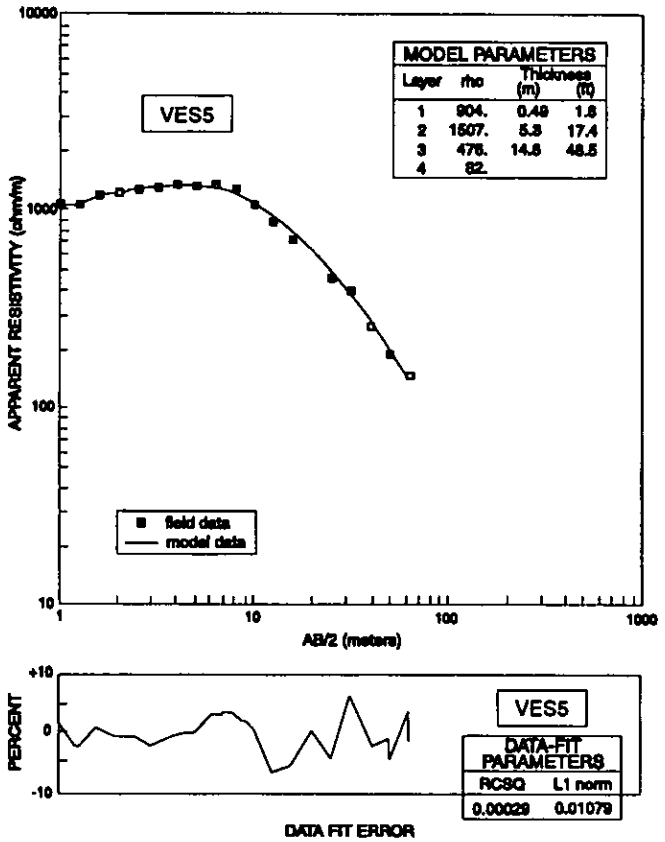

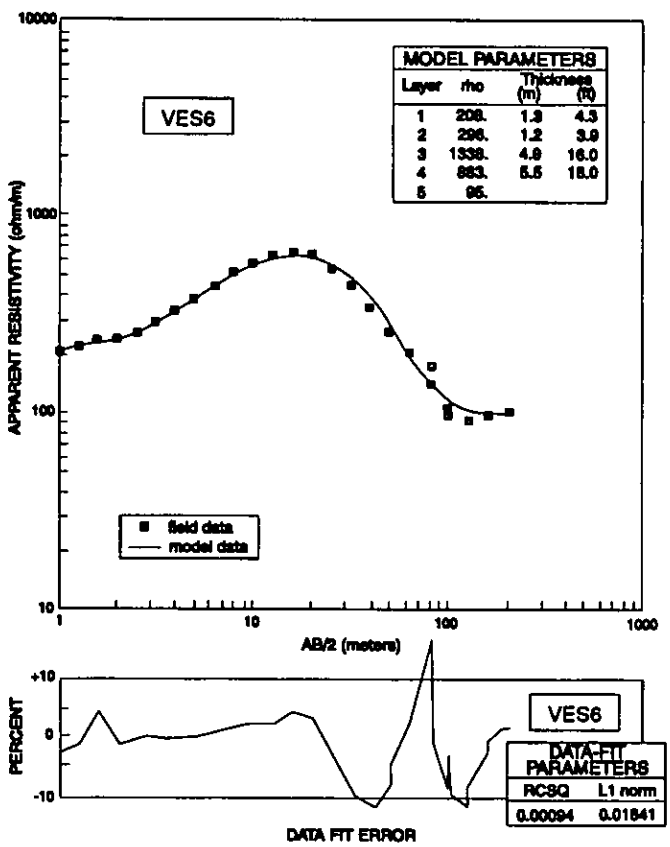

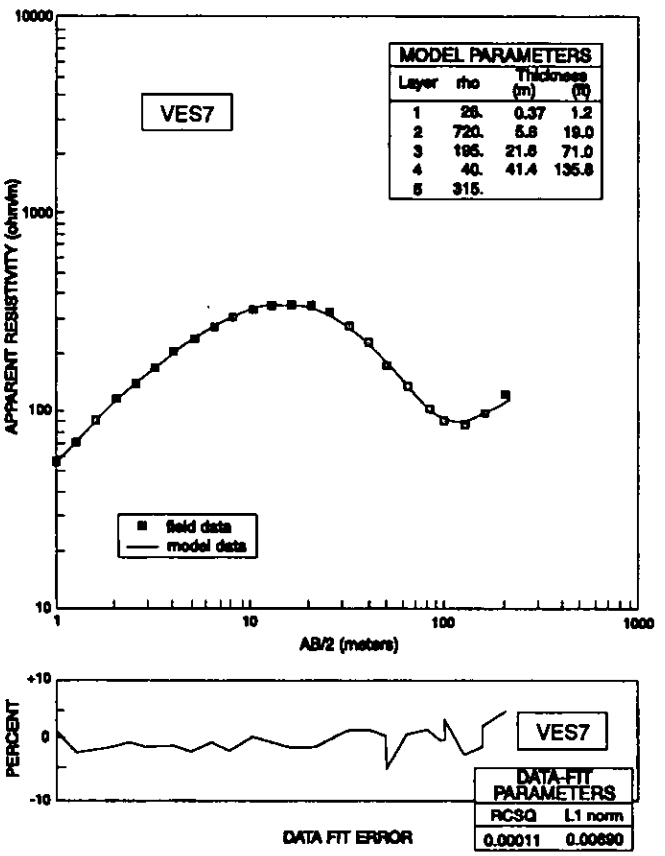

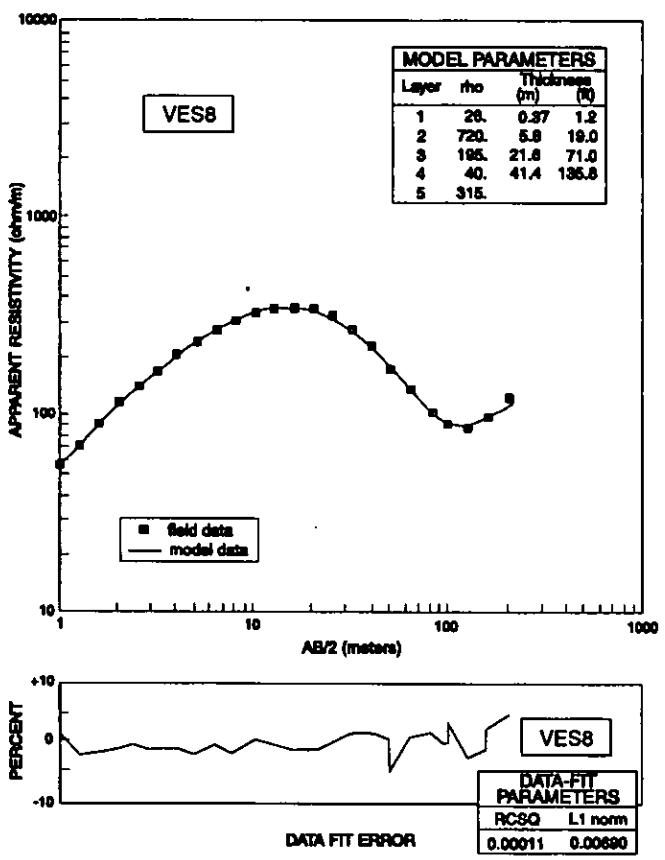

APPENDIX 1-- continued

Resistivity and induced polarization (IP) sounding interpretations showing data-fit and layer parameters.

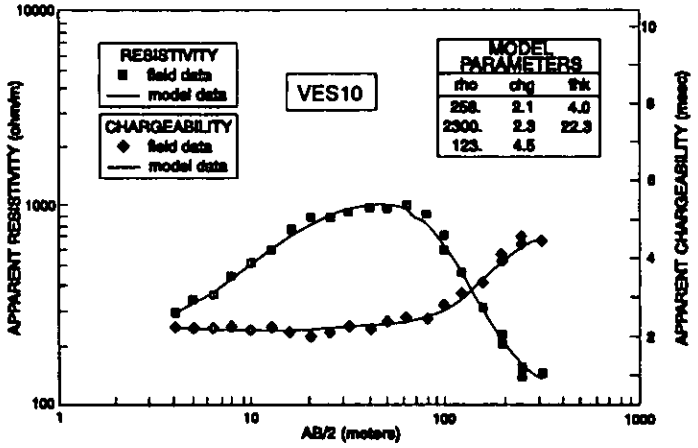

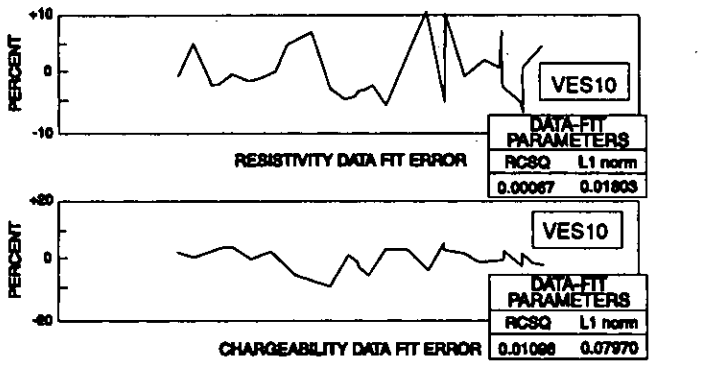

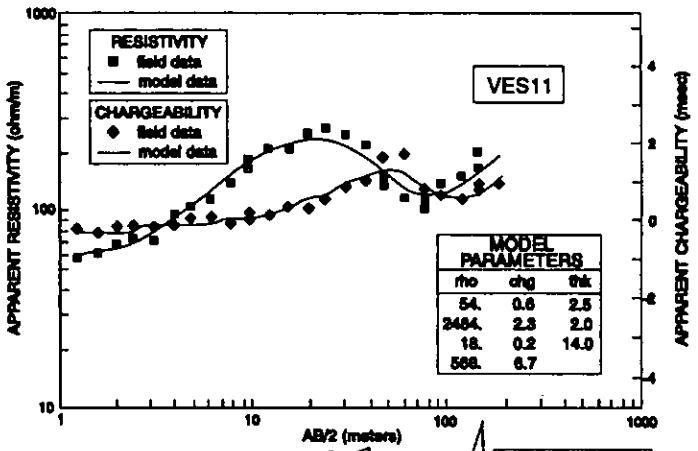

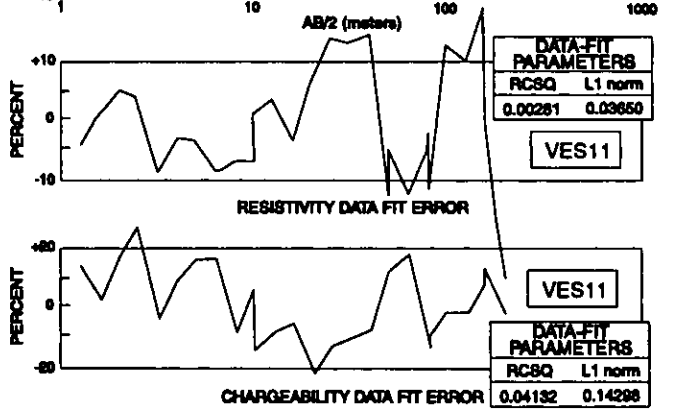

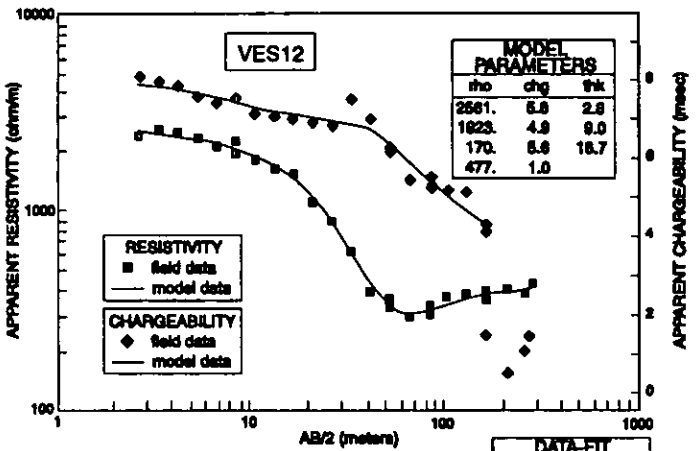

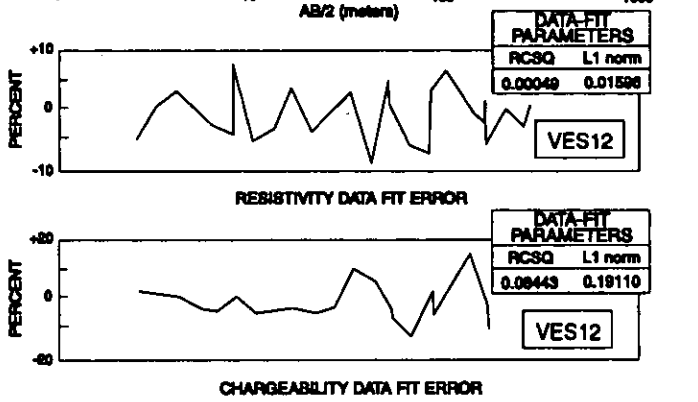

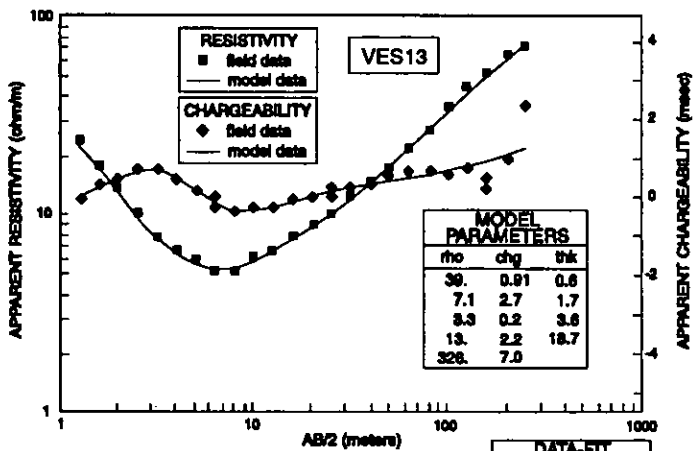

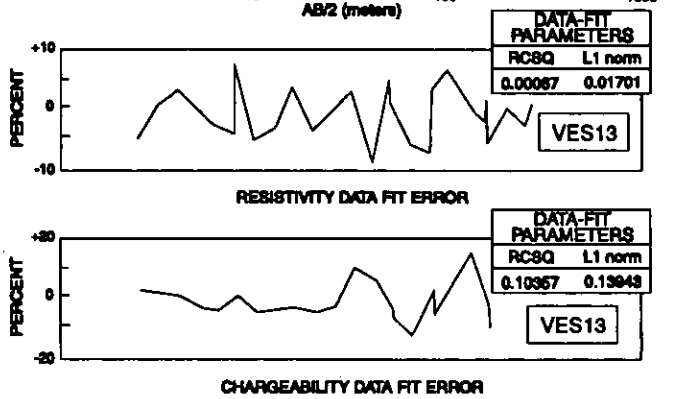

APPENDIX 1-- continued

Resistivity and induced polarization (IP) sounding interpretations showing data-fit and layer parameters.

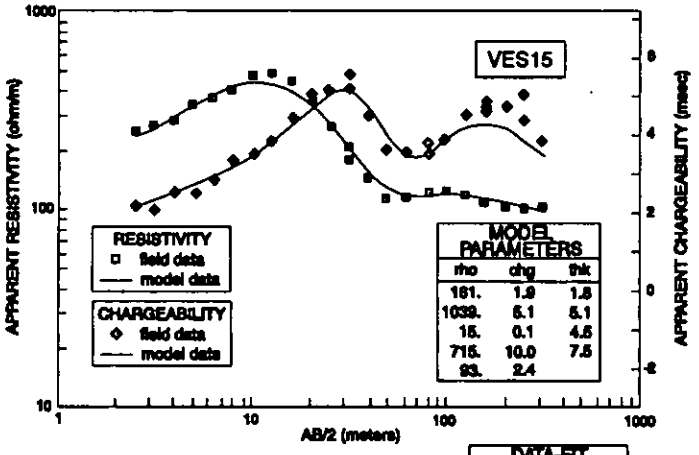

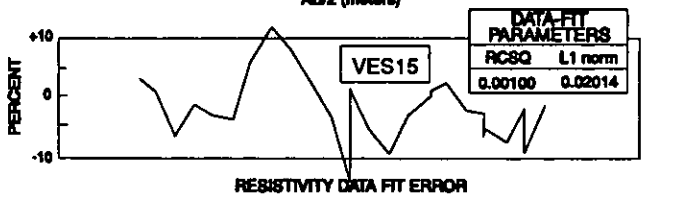

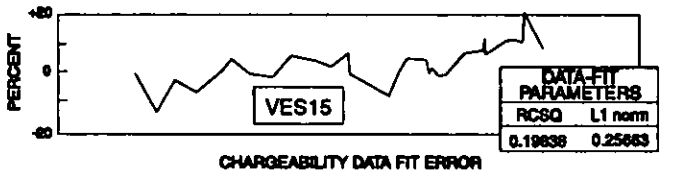

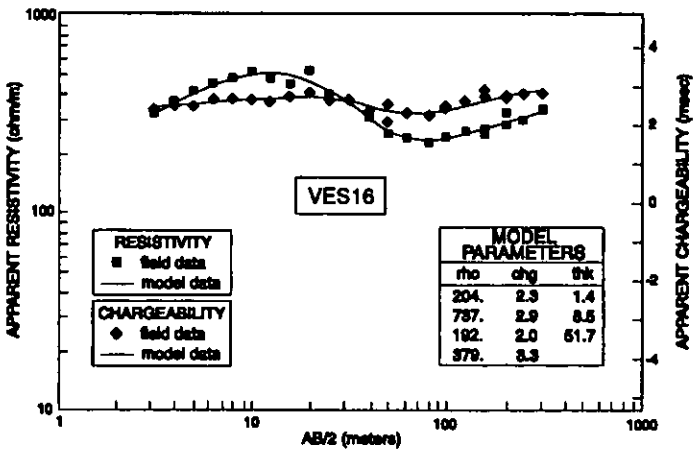

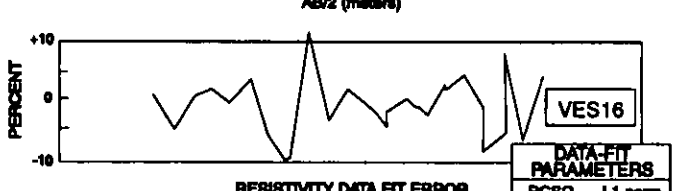

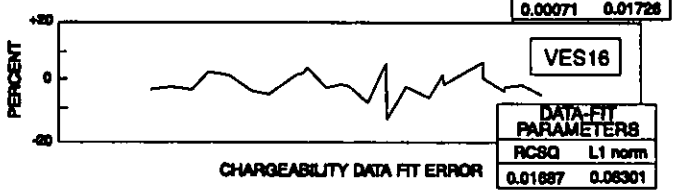

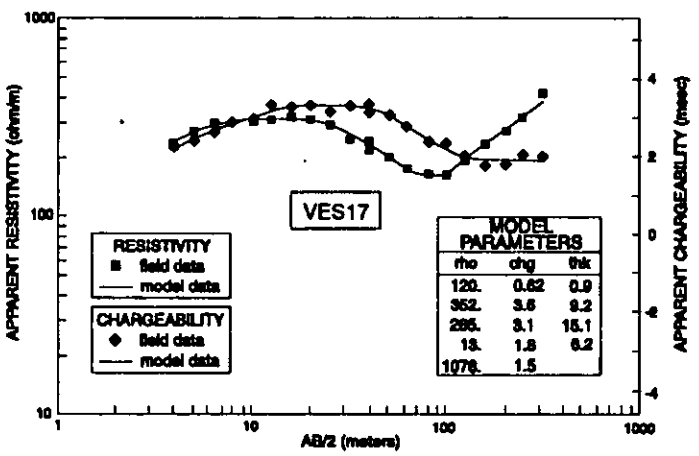

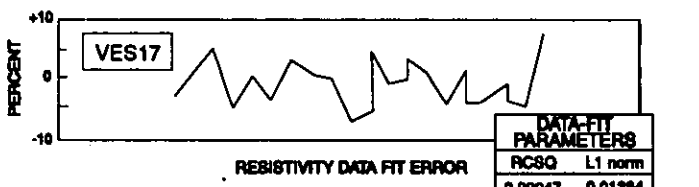

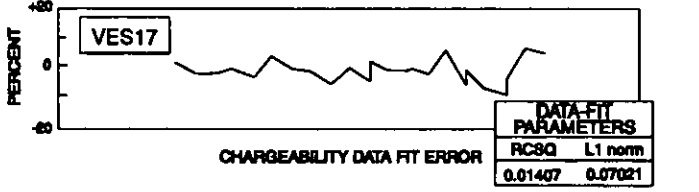

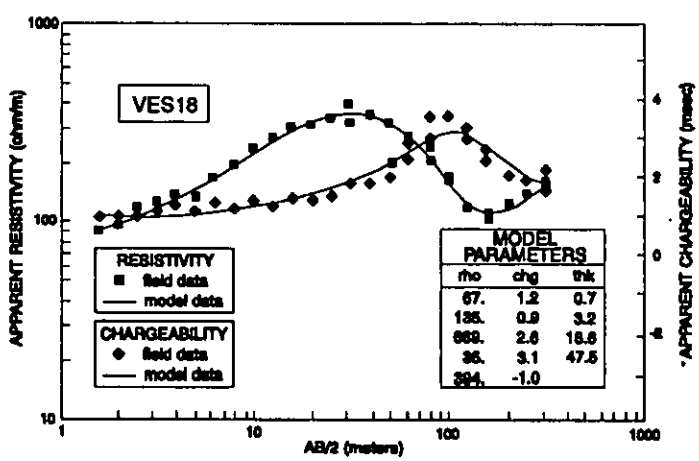

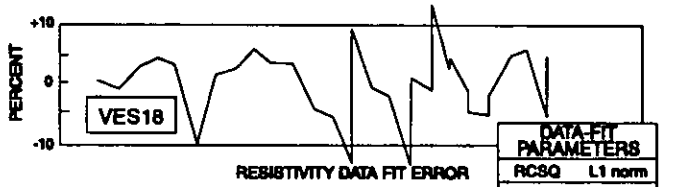

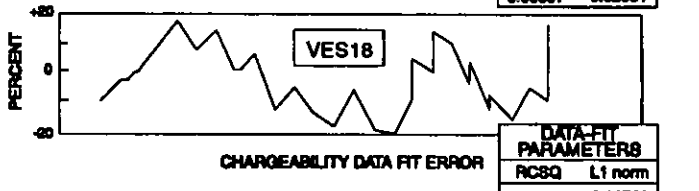

APPENDIX 1-- continued

Resistivity and induced polarization (IP) sounding interpretations showing data-fit and layer parameters.

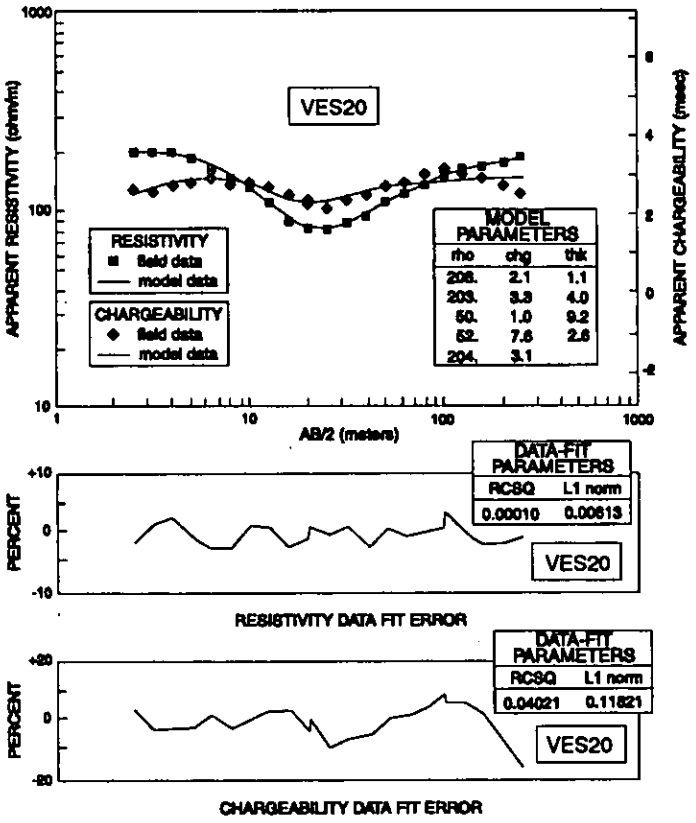

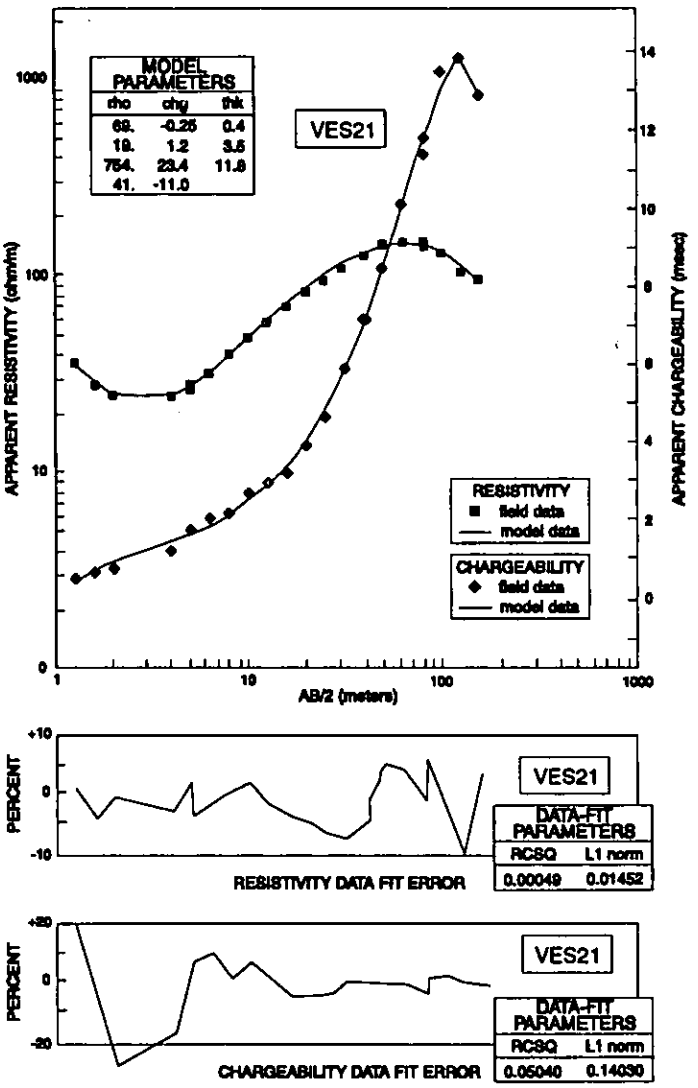

APPENDIX 1-- continued

Wenner resistivity sounding interpretations showing data-fit and layer parameters.

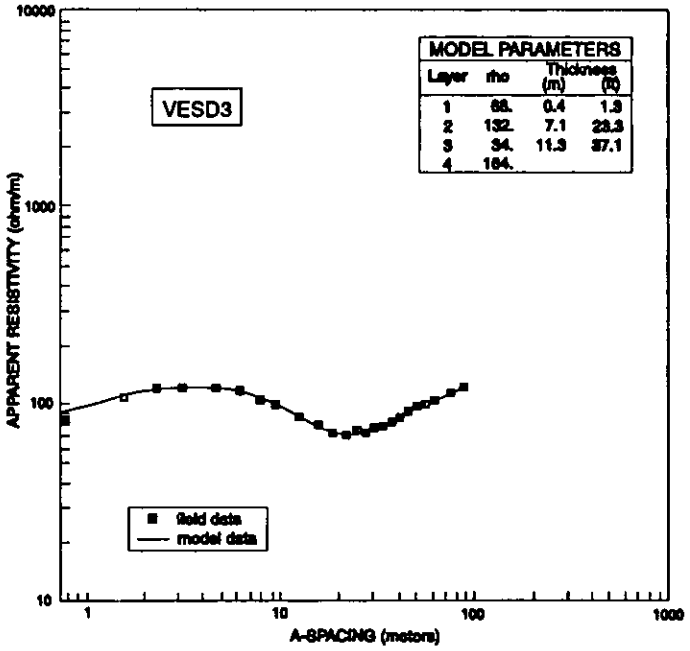

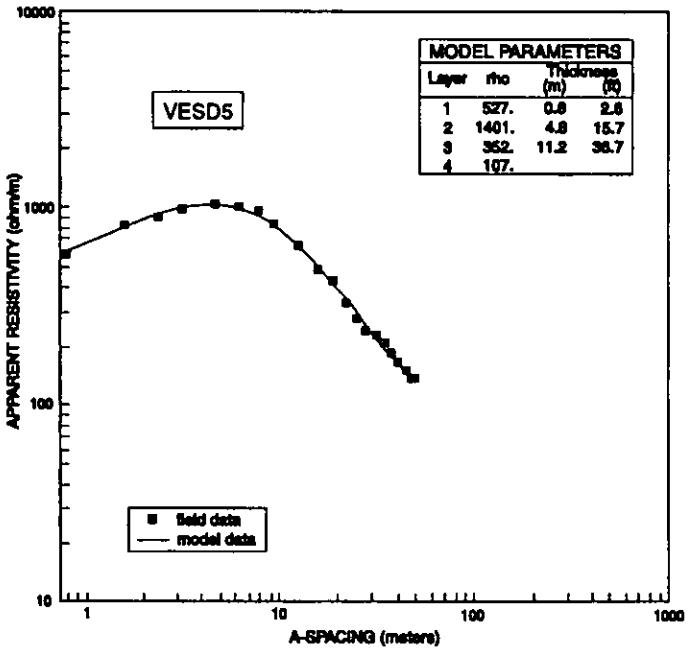

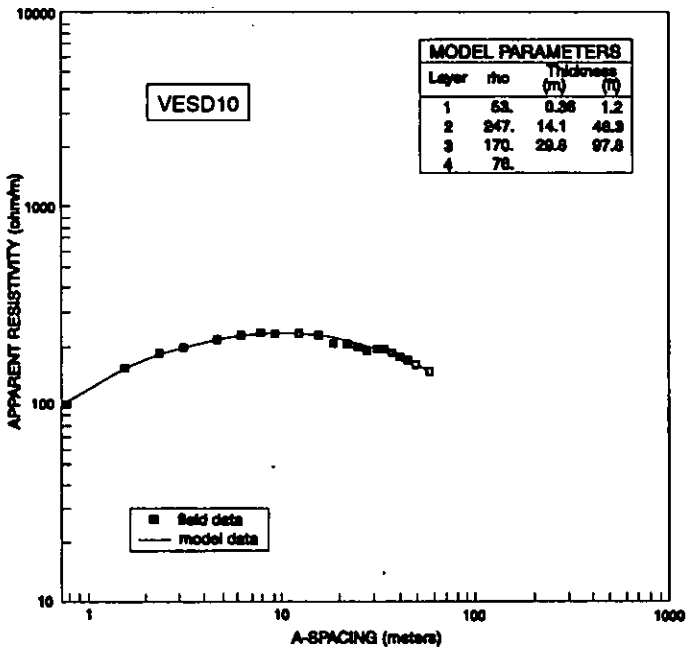

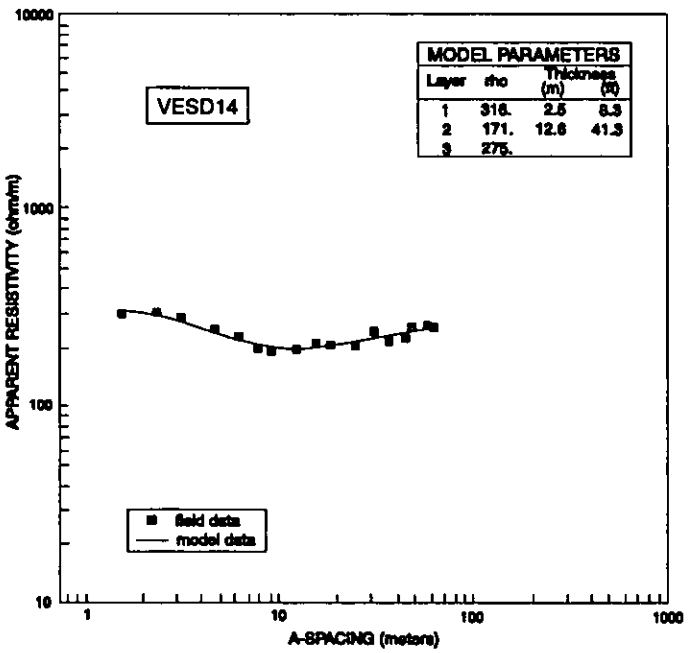

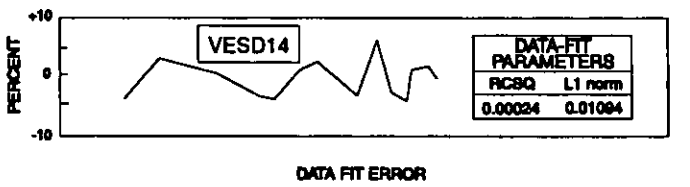

APPENDIX 2

Diurnally corrected magnetic data

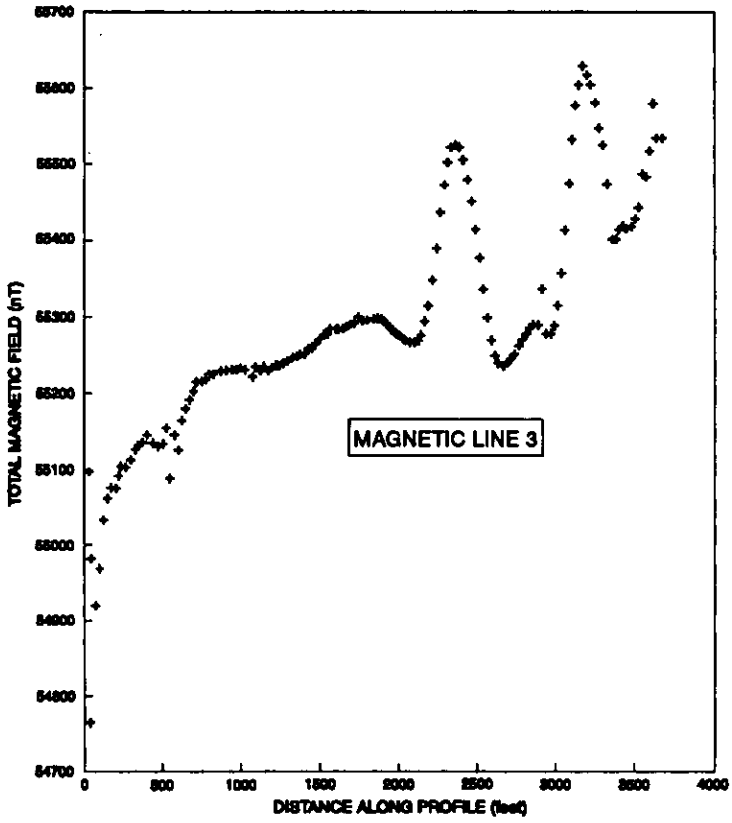

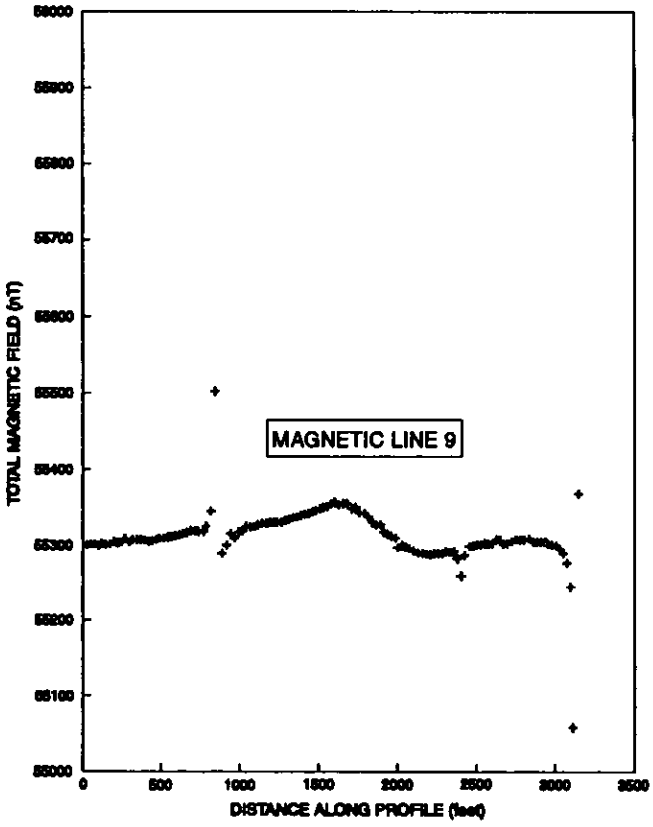

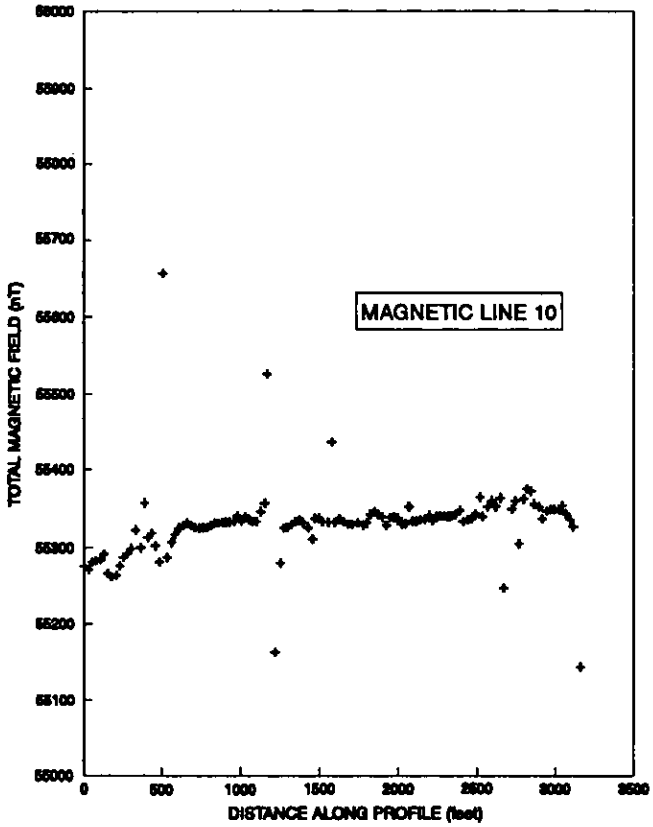

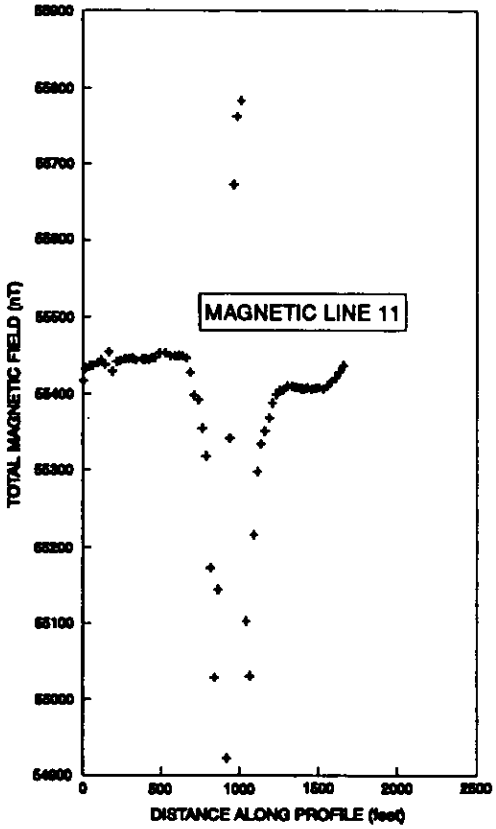

GLOSSARY

Accelerometer - see geophone

Apparent chargeability - A measured value of the time domain (IP) effect from field equipment.

Apparent resistivity - The ground resistivity based on a known current and a geometric factor derived from the assumption that the ground is homogeneous and isotropic.

Centimeter-gram-second (cgs) - Units of measurement used for some geophysical work (as opposed to the SI or MKS system of units); cgs units are mostly found in the older literature.

Chargeability - Unit of measurement for induced polarization (IP). The ratio of initial decay voltage to primary voltage in the time domain.

Geophone - An instrument used to transform seismic energy into an electrical voltage. Most land geophones are of the moving-coil type. A geophone whose output is proportional to acceleration is called an accelerometer.

Gravity method - A geophysical technique based on measurements of the earth's gravitational field. The objective in exploration work is to associate variations in gravity with differences in the distribution of densities, and hence of rock types.

Ground-Water Site Inventory (GWSI) - A U.S. Geological Survey system of numbering wells. The first two digits are the county code; numbers are assigned sequentially as wells are entered into the GWSI system.

Induced polarization (IP) - An exploration method involving measurement of the slow decay of voltage in the ground following the cessation of an excitation current pulse. In this report, the term refers particularly to membrane polarization of the earth. The unit of measurement in this study is the millisecond (ms), equivalent to the millivolt-second/volt (mV·s/V) used in some of the older literature.

Magnetic method - A geophysical technique based on measurements of the earth's magnetic field, usually with the objective of locating concentrations of magnetic materials.

Magnetic susceptibility - A measure of the degree to which a substance may be magnetized. The common unit is measured in the cgs system and is dimensionless.

Millisecond (ms) - 1/1000 of a second; time unit used in seismic methods.

Ohm-meter (ohm-m) - resistivity unit of measurement which includes cross sectional area as well as electrical resistance.

Resistivity - The capacity of a material to resist the flow of electrical current. The ratio of electric-field intensity to current density. The standard unit of measurement is the ohm-meter (ohm-m).

Resistivity method - A geophysical method based on observations of electric fields caused by current introduced into the ground.

Schlumberger electrode array - Electrode arrangement used in resistivity surveying. It consists of four collinear electrodes where the outer two serve as current sources and the inner two, closely spaced about the midpoint of the outer pair, serve as potential measuring points.

Seismic reflection method - A geophysical method based on measurement of acoustic waves reflected back to the surface from a subsurface point. The subsurface reflection point is generally located on an interface between two media of differing acoustic velocity and/or density. Velocities and thicknesses of the various media are determined from field measurements, and geologic interpretations are based on them.

Seismic refraction method - A geophysical method based on measurement of acoustic waves refracted from a geologic interface back up to the surface. Velocities and thicknesses of the various media are determined from field measurements, and geologic interpretations are based on them.

Subcrop - A buried bedrock surface beneath an unconformity.

GEOPHYSICAL INVESTIGATION OF THE POTOMAC-RARITAN-MAGOTHY AQUIFER SYSTEM AND UNDERLYING BEDROCK IN PARTS OF MIDDLESEX AND MERCER COUNTIES, NEW JERSEY
(New Jersey Geological Survey Report GSR 37)

ISSN 0741-7357

DEPARTMENT OF ENVIRONMENTAL PROTECTION
DIVISION OF SCIENCE AND RESEARCH
NEW JERSEY GEOLOGICAL SURVEY

GEOPHYSICAL INVESTIGATION OF THE POTOMAC-RARITAN-MAGOTHY AQUIFER SYSTEM AND UNDERLYING BEDROCK IN PARTS OF MIDDLESEX AND MERCER COUNTIES, NEW JERSEY
GEOLOGICAL SURVEY REPORT GSR 37
PLATE 1

EXPLANATION

- **Bedrock geologic contact** - based on drillers' logs and geophysical investigations.
- **Bedrock elevation contour** - contour interval 25 feet; dashed where approximately located.
- VES19 **Resistivity/Induced Polarization(IP) line**
- -188 SSR33 -222 **Seismic line** - interpreted bedrock elevation at each end of the line.
- magnetic line 10 **Magnetic line** - stations omitted because of close spacing.
- +11 **Gravity station**
- 230191 TD-223 **Well** - ground water site inventory number (GWSI), bedrock elevation, or elevation of total depth (TD) drilled.
- 230431 -121 basalt **Well** - drilled into bedrock.

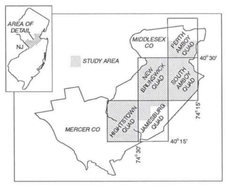

SCALE 1:24000

1 mile
1000 0 1000 2000 3000 4000 5000 6000 7000 feet
1 kilometer

BASE MAP CONTOUR INTERVAL 20 FEET (NEW BRUNSWICK & SOUTH AMBOY QUADRANGLES)
BASE MAP CONTOUR INTERVAL 10 FEET (PERTH AMBOY QUADRANGLE)
DATUM IS MEAN SEA LEVEL

NEWARK SUPERGROUP (sedimentary bedrock)
NEWARK SUPERGROUP (diabase)
NEWARK SUPERGROUP (sedimentary bedrock)
UNKNOWN BODY
CRYSTALLINE BEDROCK

Cartography by Z. Allen-Lafayette

PLATE 1. Bedrock topography, rock type, and locations of well data and geophysical data in parts of the New Brunswick, South Amboy, and Perth Amboy Quadrangles, Middlesex County, New Jersey

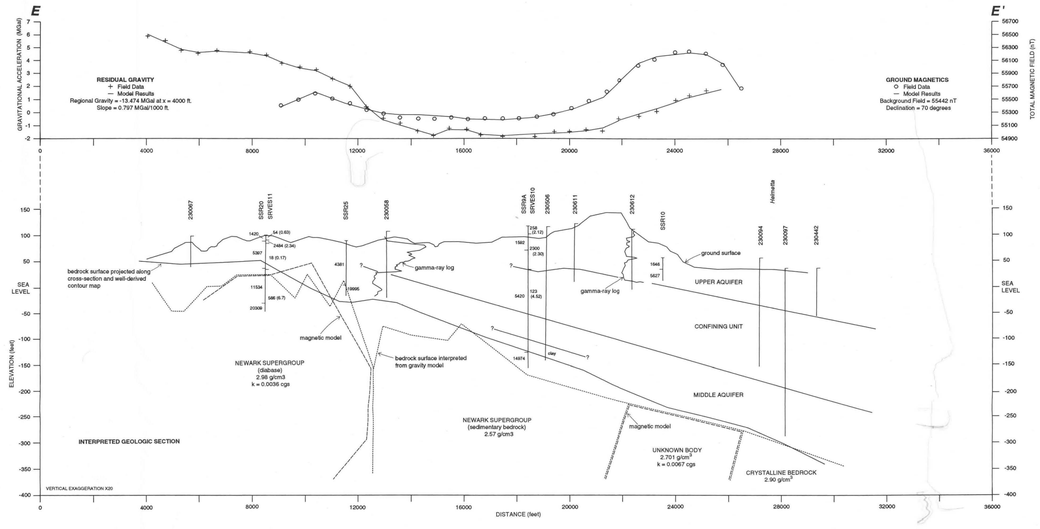

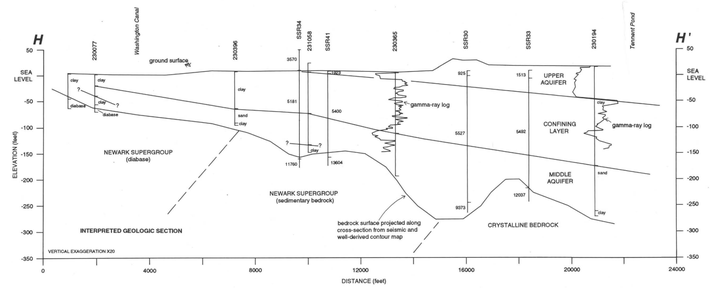

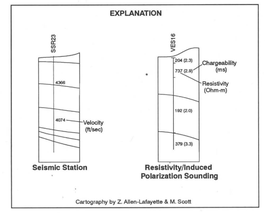

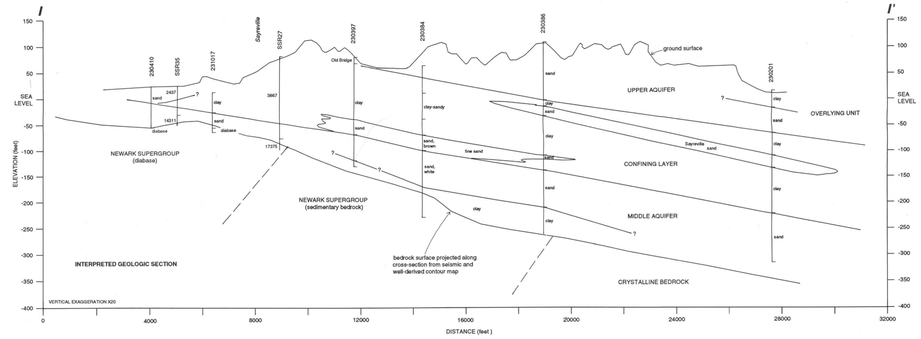

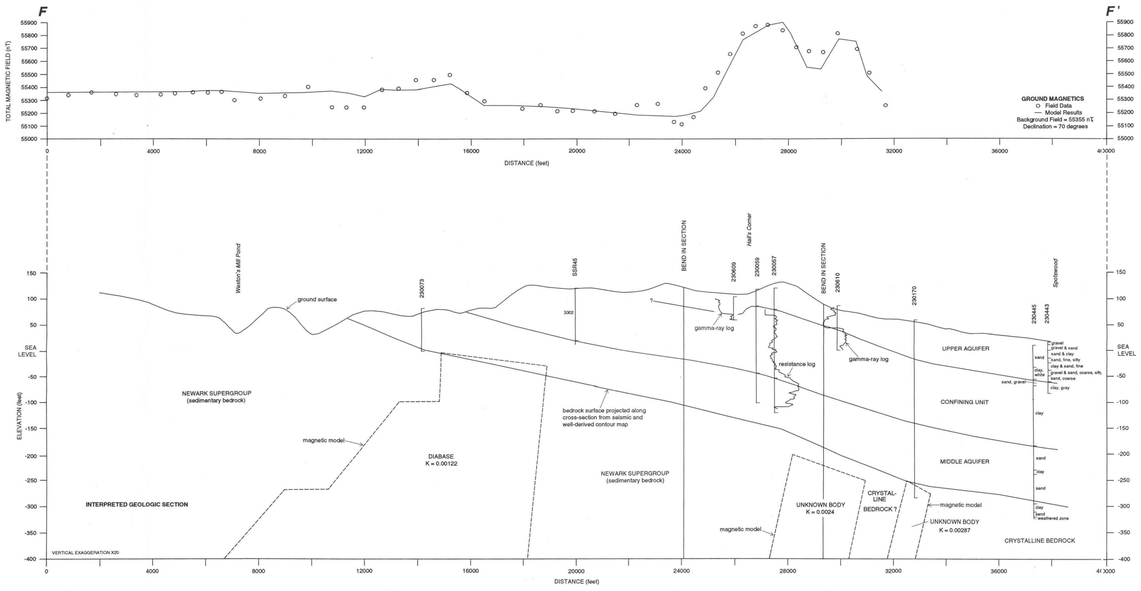

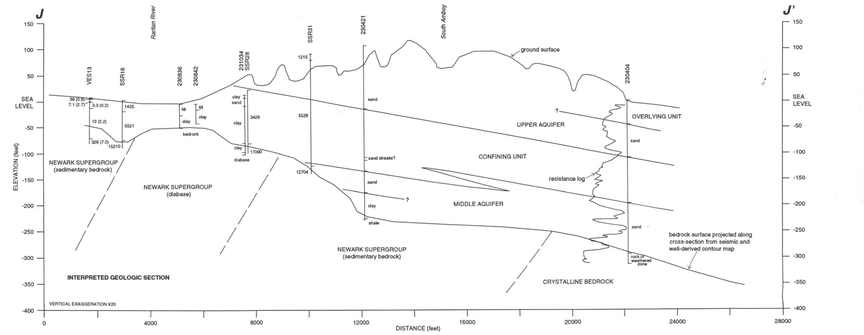

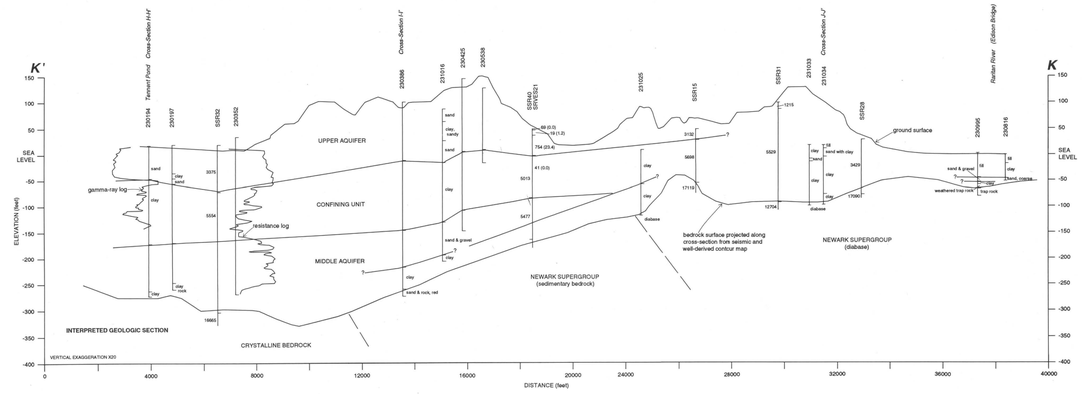

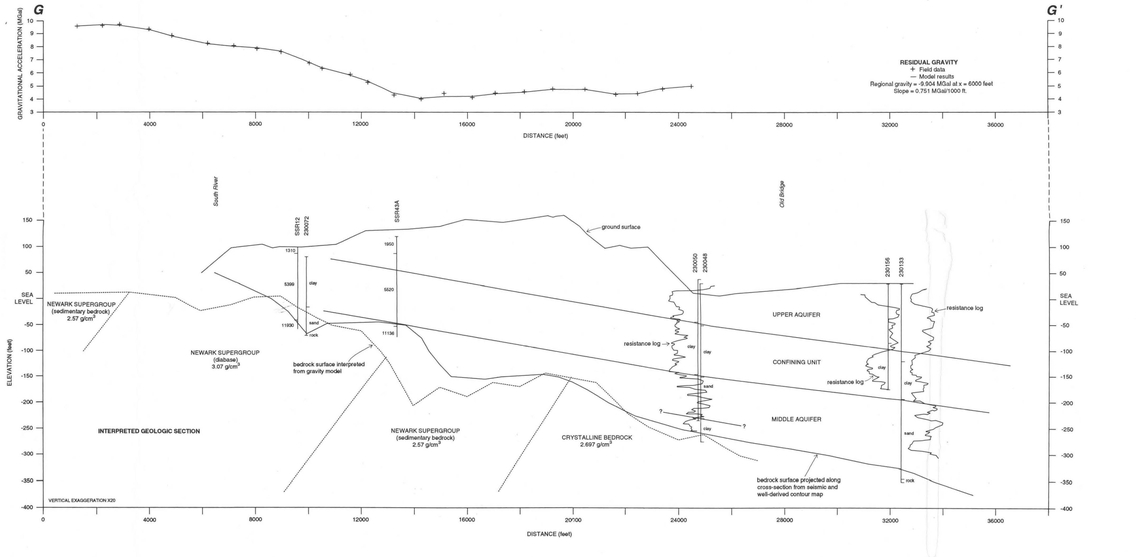

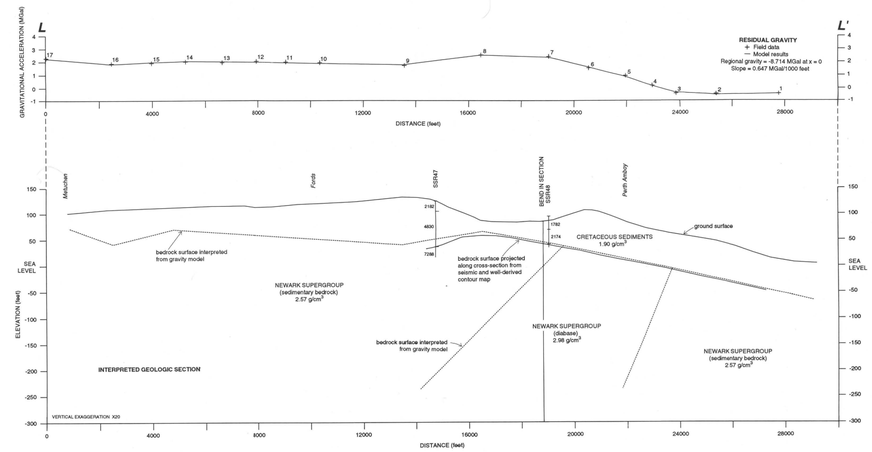

PLATE 2. Geophysical data and interpreted geologic sections *E-E'* through *L-L'* accompanying Plate 1

DEPARTMENT OF ENVIRONMENTAL PROTECTION
DIVISION OF SCIENCE AND RESEARCH
NEW JERSEY GEOLOGICAL SURVEY

GEOPHYSICAL INVESTIGATION OF THE POTOMAC-RARITAN-MAGOTHY AQUIFER SYSTEM AND UNDERLYING BEDROCK IN PARTS OF MIDDLESEX AND MERCER COUNTIES, NEW JERSEY
GEOLOGICAL SURVEY REPORT GSR 37
PLATE 3

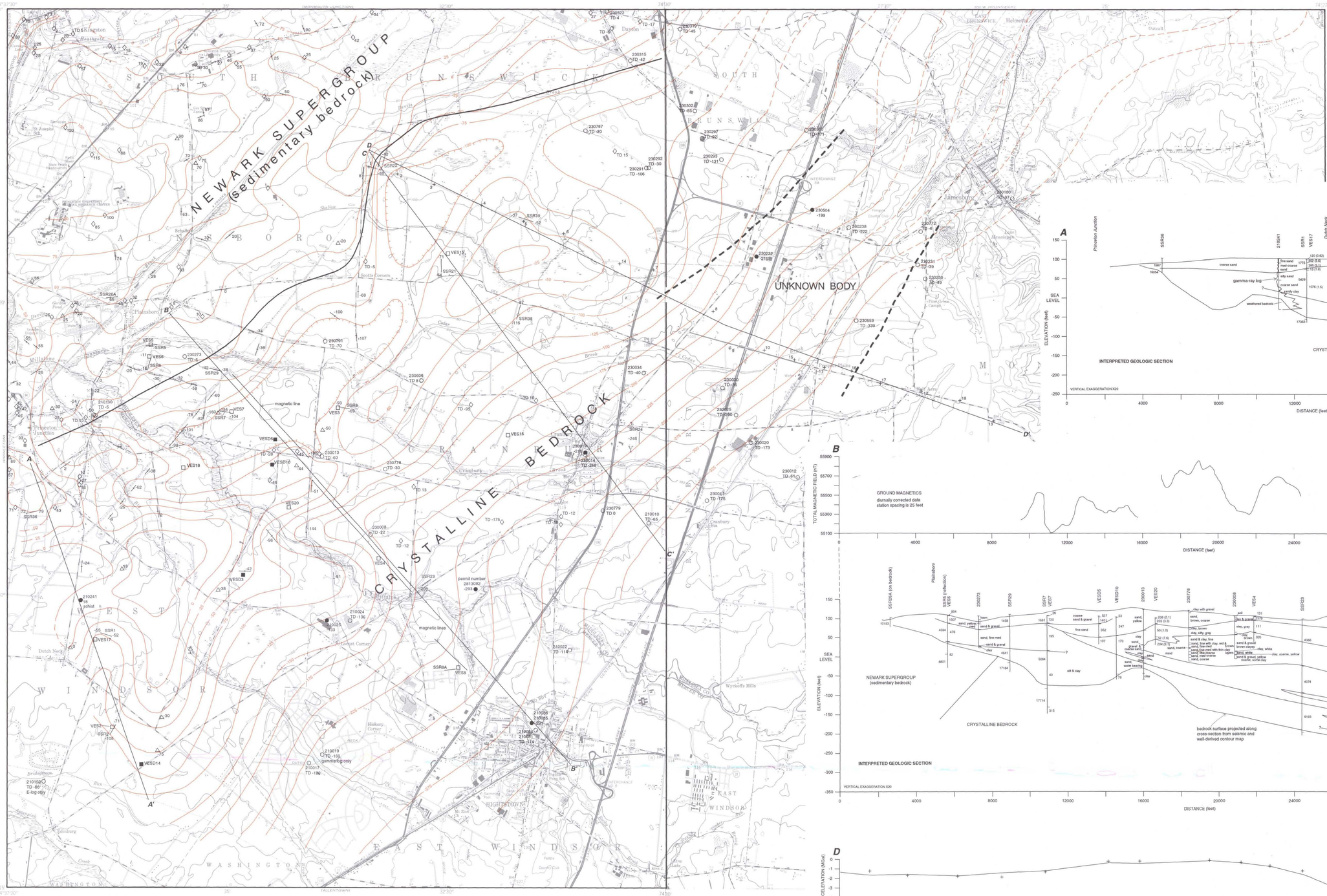

SCALE 1:24000

1 1/2 0 1 mile

1000 0 1000 2000 3000 4000 5000 6000 7000 feet

1 1/2 0 1 kilometer

BASE MAP CONTOUR INTERVAL 20 FEET
DATUM IS MEAN SEA LEVEL

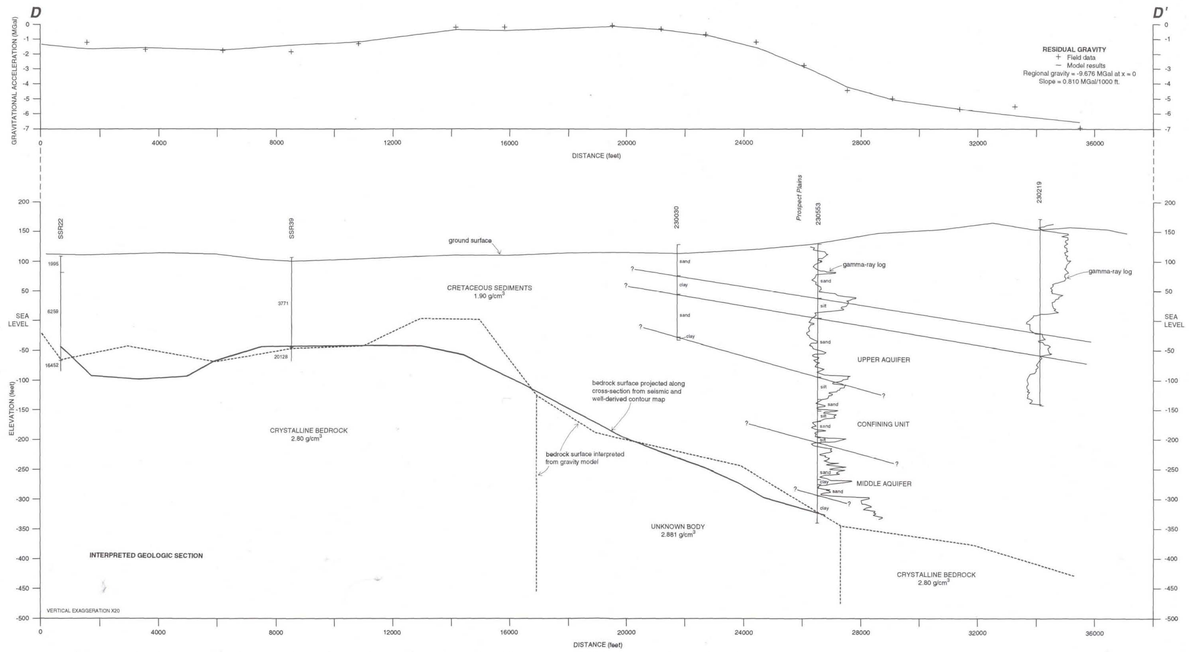

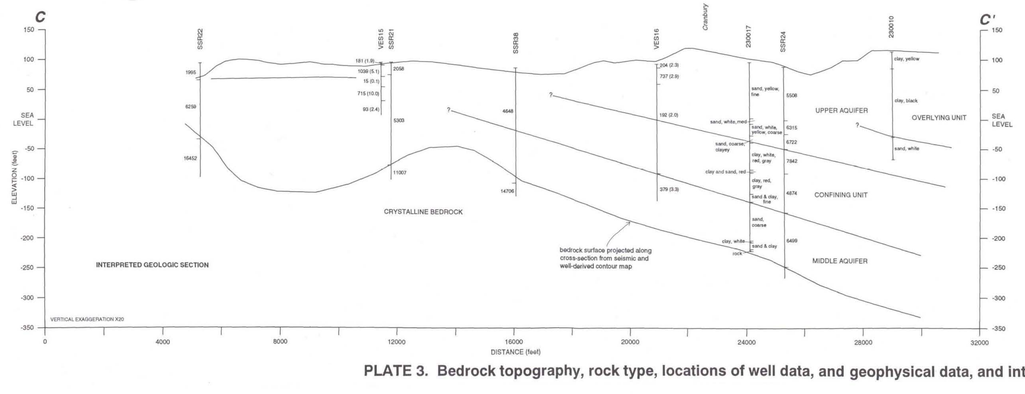

EXPLANATION

- **Bedrock geologic contact** - based on drillers' logs and geophysical investigations.
- **Bedrock elevation contour** - contour interval 25 feet; dashed where approximately located.
- VES16 **Resistivity/Induced Polarization(IP) line**
- VESD3 **Wenner resistivity sounding** (Dudley's Princeton thesis, 1960).
- SSR33 **Seismic line** - interpreted bedrock elevation at each end of the line.
- **Seismic line** with interpreted bedrock elevation (Runyon's Princeton thesis, 1961).
- **Seismic line** with interpreted bedrock elevation (Yahn's Princeton thesis, 1945).
- **Magnetic line** - stations omitted because of close spacing.
- **Gravity station**
- **Well** - ground water site inventory number (GWSI), bedrock elevation, or elevation of total depth (TD) drilled.
- **Well** - drilled into bedrock.
- **Well** - elevation of bedrock or elevation of total depth (TD) drilled (Runyon's Princeton thesis, 1961).

PLATE 3. Bedrock topography, rock type, locations of well data, and geophysical data, and interpreted geologic sections *A-A'* through *D-D'* in the Hightstown and part of the Jamesburg Quadrangles, Mercer and Middlesex Counties, New Jersey

Cartography by Z. Allen-Lafayette & M. Scott